

NASA-CR-172366

NASA Contractor Report 172366

NASA-CR-172366
19850005492

**An In-Flight Investigation of a
Twin Fuselage Configuration in
Approach and Landing**

Norman C. Weingarten

**ARVIN/CALSPAN Advanced Technology Center
Buffalo, N.Y. 14225**

**Purchase Order L-61966B
August 1984**

NASA
National Aeronautics and
Space Administration

**Langley Research Center
Hampton, Virginia 23665**

LIBRARY COPY

1984

**LANGLEY RESEARCH CENTER
LIBRARY, NASA
HAMPTON, VIRGINIA**

ERRATA

*CR No changed
12-18-84*

NASA Contractor Report 172366

AN IN-FLIGHT INVESTIGATION OF A TWIN FUSELAGE
CONFIGURATION IN APPROACH AND LANDING

Norman C. Weingarten
ARVIN/CALSPAN Advanced Technology Center

August 1984

NASA Contractor Report 172337 was erroneously printed on the cover and Report Documentation Page of this document.

The correct report number is NASA Contractor Report 172366. The report number should be changed on the cover and in Block 1 of the Report Documentation Page.

Issued 12-14-84



FOREWORD

This report was prepared for the National Aeronautics and Space Administration, Langley Research Center, Hampton, Virginia by Arvin/Calspan Advanced Technology Center, Buffalo, New York. It covers the preparation, conduct, and analysis of an in-flight simulation program investigating the flying qualities of a Twin-Fuselage aircraft design. The aircraft used was the USAF/AFWAL Total In-Flight Simulator (TIFS) which is operated by Calspan under Air Force Contract No. F33615-79-C-3618 and F33615-83-C-3603. The program was sponsored by NASA and administered by USAF/AFWAL.

Mr. William Grantham was the Project Manager for NASA/LRC and Capt. Michael Maroney was the Program Manager for AFWAL.

The work reported here was performed by the Flight Research Department of Calspan. Dr. Philip Reynolds was the Program Manager for the overall TIFS program. Mr. Robert Radford was the Project Engineer for this task. Mr. Norman Weingarten was responsible for the analysis and reporting. The evaluation pilots were Kenneth R. Yenni from NASA/LRC and Major William R. Neely, Jr. from USAF.

The author wishes to acknowledge the contributions of individuals who participated in this program: Mr. Charles Chalk, who assisted in the experiment design; Messrs. Charles Berthe, Michael Parrag and John Ball, safety pilots; Messrs. Robert Gavin, Ralph Siracuse and James Dittenhauser, computer and electronic systems preparation; Ms. Chris Turpin, report preparation.



TABLE OF CONTENTS

<u>Section</u>	<u>Title</u>	<u>Page</u>
1	INTRODUCTION.	1-1
2	EXPERIMENT DESIGN	2-1
	2.1 AIRCRAFT MODEL	2-1
	2.2 CONFIGURATIONS	2-15
	2.3 TEST DESCRIPTION	2-20
	2.3.1 Introduction.	2-20
	2.3.2 Evaluation Tasks and Procedures	2-21
	2.3.3 Pilot Comment Card and Rating Scale	2-22
	2.3.4 Evaluation Pilots	2-22
3	EXPERIMENT MECHANIZATION.	3-1
	3.1 EQUIPMENT.	3-1
	3.2 SIMULATION GEOMETRY AND TRANSFORMATION EQUATIONS	3-6
	3.3 CROSSWIND SIMULATION	3-11
	3.4 DATA RECORDED.	3-11
4	RESULTS	4-1
	4.1 INTRODUCTION	4-1
	4.2 EVALUATION CHRONOLOGY.	4-1
	4.3 PILOT RATING AND COMMENT SUMMARY	4-6
	4.4 POST-FLIGHT WRITTEN PILOT COMMENTS	4-18
	4.5 DISCUSSION OF RESULTS.	4-22
	4.6 POTENTIAL CRITERIA FOR LATERAL PILOT OFFSET POSITION EFFECTS	4-25
	4.7 MODEL FOLLOWING FIDELITY EFFECTS	4-26
	4.8 CONCLUSIONS AND RECOMMENDATIONS.	4-32
5	REFERENCES.	5-1
 <u>Appendix</u>		
A	MODEL FOLLOWING CONTROL ALGORITHMS.	A-1



LIST OF TABLES

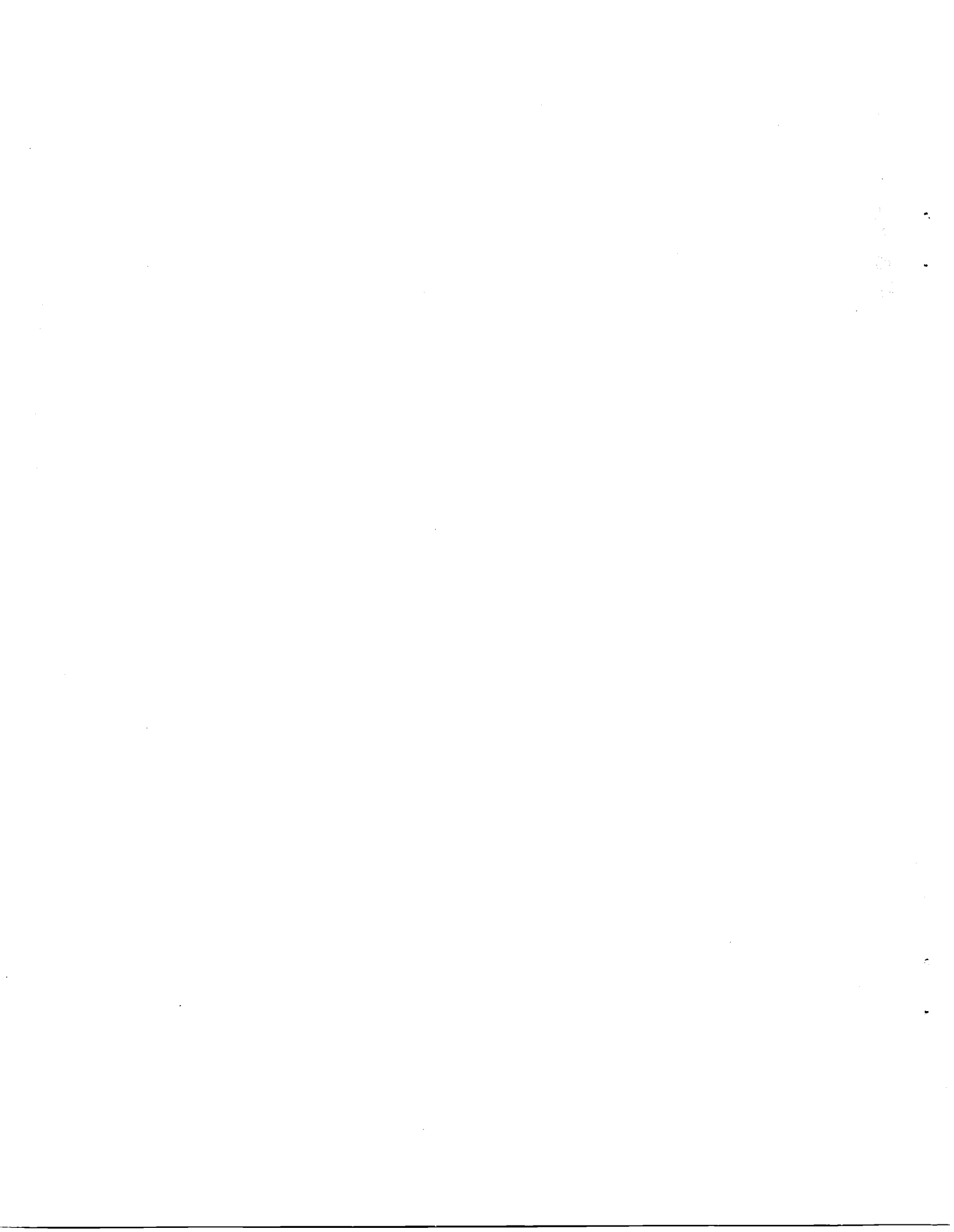
<u>Table</u>	<u>Title</u>	<u>Page</u>
1	TWIN FUSELAGE PHYSICAL CHARACTERISTICS AND TRIM CONDITIONS . . .	2-3
2	TWIN FUSELAGE NON-DIMENSIONAL STABILITY AND CONTROL DERIVATIVES.	2-4
3	NON LINEAR $C_D(\alpha)$ AND $C_m(\alpha)$	2-5
4	GROUND EFFECT.	2-5
5	FEEL SYSTEM AND CONTROLLER CHARACTERISTICS	2-11
6	FLYING QUALITIES CHARACTERISTICS	2-20
7	DIGITAL RECORDING LIST	3-12
8	NORMAL ACCELERATION PER ROLL RATE PARAMETER.	4-25

LIST OF FIGURES

<u>Figure</u>	<u>Title</u>	<u>Page</u>
1	GENERAL TWIN FUSELAGE TRANSPORT ARRANGEMENT.	2-2
2	LONGITUDINAL CONTROL SYSTEM.	2-6
3	ROLL CONTROL SYSTEM.	2-7
4	YAW CONTROL SYSTEM	2-9
5	AUTO THROTTLE.	2-10
6	PITCH RATE AND N_{z_p} RESPONSE TO STEP INPUT.	2-16
7	ROLL RATE AND N_{z_p} RESPONSE TO STEP INPUT, SCAS-1	2-17
8	ROLL RATE AND N_{z_p} RESPONSE TO STEP INPUT, SCAS-2	2-18
9	ROLL RATE AND N_z RESPONSE TO STEP INPUT, SCAS-3.	2-19
10	PILOT COMMENT CARD	2-23
11	COOPER-HARPER HANDLING QUALITIES RATING SCALE.	2-24
12	PIU TENDENCY CLASSIFICATION.	2-25
13	USAF/CALSPAN TOTAL IN-FLIGHT SIMULATOR (TIFS).	3-3
14	TIFS MODEL FOLLOWING SIMULATION.	3-4
15	TIFS EVALUATION COCKPIT.	3-5
16	CAPTAIN'S INSTRUMENT PANEL IN EVALUATION COCKPIT	3-5
17	PILOT RATING VERSUS PILOT POSITION, ($\tau_R = 0.6$ sec)	4-12
18	PILOT RATING VERSUS PILOT POSITION, ($\tau_R = 1.2$ sec)	4-13
19	PILOT RATING VERSUS PILOT POSITION, ($\tau_R = 2.3$ sec)	4-14
20	PILOT RATING VERSUS τ_R , ($Y_p = 0$ ft).	4-15
21	PILOT RATING VERSUS τ_R , ($Y_p = 30$ ft)	4-16
22	PILOT RATING VERSUS τ_R , ($Y_p = 50$ ft)	4-17
23	MODEL FOLLOWING, FLT 750, APPROACH 4, SCAS-2, $Y_p = 50$ FT	4-27
24	MODEL FOLLOWING, FLT 750, APPROACH 7, SCAS-1, $Y_p = 30$ FT	4-28
25	MODEL FOLLOWING, FLT 750, APPROACH 9, SCAS-1, $Y_p = 50$ FT	4-29
26	MODEL FOLLOWING WITH V ERROR AND THROTTLE SURGING, FLT750 APPROACH 9, SCAS-1, $Y_p = 50$ FT	4-31

TABLE OF SYMBOLS

b	span	<u>Subscripts</u>	
\bar{c}	mean chord	a	aileron
C_D, C_L, C_Y	force coefficients in stability axes	CG	center of gravity
C_{ℓ}, C_m, C_n	moment coefficients in body axes	d	refers to the denominator of the ϕ/δ_a transfer function
g	gravitational constant	e	elevator
h	altitude	GE	ground effect
m	mass	h	horizontal tail
n	accelerometer output	LG	landing gear
p, q, r	body axis angular rates	M,m	model
u, v, w	body axis linear velocities	MF	model following
x, y, z	body axis distance	MTCG	model CG to TIFS CG
I	moment of inertia	p	pilot
S	wing area	ph	phugoid
T	thrust	PMCG	model CG to pilot
V	true airspeed	PTCG	TIFS CG to pilot
α	angle of attack	r	rudder
β	sideslip angle	SP	spoiler or short period
γ	flight path angle	T	TIFS
δ	control surface deflection damping ratio	ϕ	refers to numerator of the ϕ/δ_a transfer function
θ	pitch angle	<u>Other Notations</u>	
τ	time constant	()*	refers to an axis system with origin at the model CG parallel to the TIFS body axis
ϕ	bank angle	($\dot{\quad}$)	time rate of change of ()
ω	natural frequency		



Section 1
INTRODUCTION

Experiments performed in the USAF-AFWAL Total In-Flight Simulator (TIFS), (References 1 and 2) have shown that the lateral acceleration and the normal acceleration at the pilot's station are important to the flying qualities and ride qualities of an airplane during Terminal Flight Phase operations. In Reference 1, it was shown that the lateral acceleration at the pilot's station, experienced during rolling and turning maneuvers, can be excessive if the roll damping is very high and the pilot is located a large distance above the X stability axis. In Reference 2, it was shown that flight path control problems can result if the pilot is located behind the center of rotation for elevator control inputs.

The linear accelerations at the pilot station of a twin-fuselage airplane will be nonlinear functions of the angular accelerations and angular velocities as indicated by the following equations:

$$\begin{aligned}
 n_{x_p} &= n_{x_{CG}} + \frac{1}{57.3g} \left[-x_p \frac{r^2+q^2}{57.3} + y_p \left(\frac{pq}{57.3} - \dot{r} \right) + z_p \left(\frac{pr}{57.3} + \dot{q} \right) \right] \\
 n_{y_p} &= n_{y_{CG}} + \frac{1}{57.3g} \left[x_p \left(\frac{pq}{57.3} + \dot{r} \right) - y_p \frac{p^2+r^2}{57.3} + z_p \left(\frac{qr}{57.3} - \dot{p} \right) \right] \\
 n_{z_p} &= n_{z_{CG}} + \frac{1}{57.3g} \left[x_p \left(\frac{pr}{57.3} - \dot{q} \right) + y_p \left(\frac{qr}{57.3} + \dot{p} \right) - z_p \frac{q^2+p^2}{57.3} \right]
 \end{aligned}$$

To simplify these equations for transport type airplanes the terms involving the angular rates squared and products of angular rates can probably be ignored. The equations then reduce to

$$\begin{aligned}
 n_{x_p} &= n_{x_{CG}} + \frac{1}{57.3g} \left[-y_p \dot{r} + z_p \dot{q} \right] \\
 n_{y_p} &= n_{y_{CG}} + \frac{1}{57.3g} \left[x_p \dot{r} - z_p \dot{p} \right] \\
 n_{z_p} &= n_{z_{CG}} + \frac{1}{57.3g} \left[-x_p \dot{q} + y_p \dot{p} \right]
 \end{aligned}$$

In Reference 1, it was shown that the term $Z_p \dot{p}$ was an important contributor to lateral acceleration when maneuvering with the ailerons and in Reference 2 it was shown that the term $X_p \dot{q}$ was important to flight path control during flare and landing. It is anticipated that the term $Y_p \dot{p}$ may be significant to the flying qualities of twin-fuselage designs where the pilot is not located in the plane of symmetry. The terms $Y_p \dot{r}$ and $X_p \dot{r}$ may be significant during the rudder pedal induced yawing maneuvers.

The National Aeronautical and Space Administration/Langley Research Center has recently performed piloted ground simulation studies of large twin-fuselage transport aircraft in which the pilot station was located in the nose of one of the two fuselages. This design configuration places the pilot a significant distance left or right of the plane of symmetry as well as being forward of the center of gravity. A consequence of this configuration is that rolling maneuvers cause vertical motions at the pilot station thus coupling the piloting cues (normally associated with pitch control) with the roll control activity. The cues of importance are both visual (altitude and rate of change of altitude) and kinetic (acceleration related).

Since visual cues available in ground simulators are marginally adequate to permit valid evaluation of flying qualities during flare and touchdown and the limited amplitude motion cues of ground simulators are quite inadequate for assessment of the effects of unusual airplane motions, it was proposed that in-flight evaluations be performed for a number of these configurations using the TIFS in-flight simulator. The description and results of the TIFS experiment are the subject of this report. The experiment was basically designed to evaluate the effects of cockpit location and augmented airplane dynamics in roll on the flying qualities for terminal area maneuvering, approach and landing. The experiment matrix was jointly defined by Camspan and NASA/LRC personnel to permit taking advantage of results from the NASA ground simulation experiment previously performed.

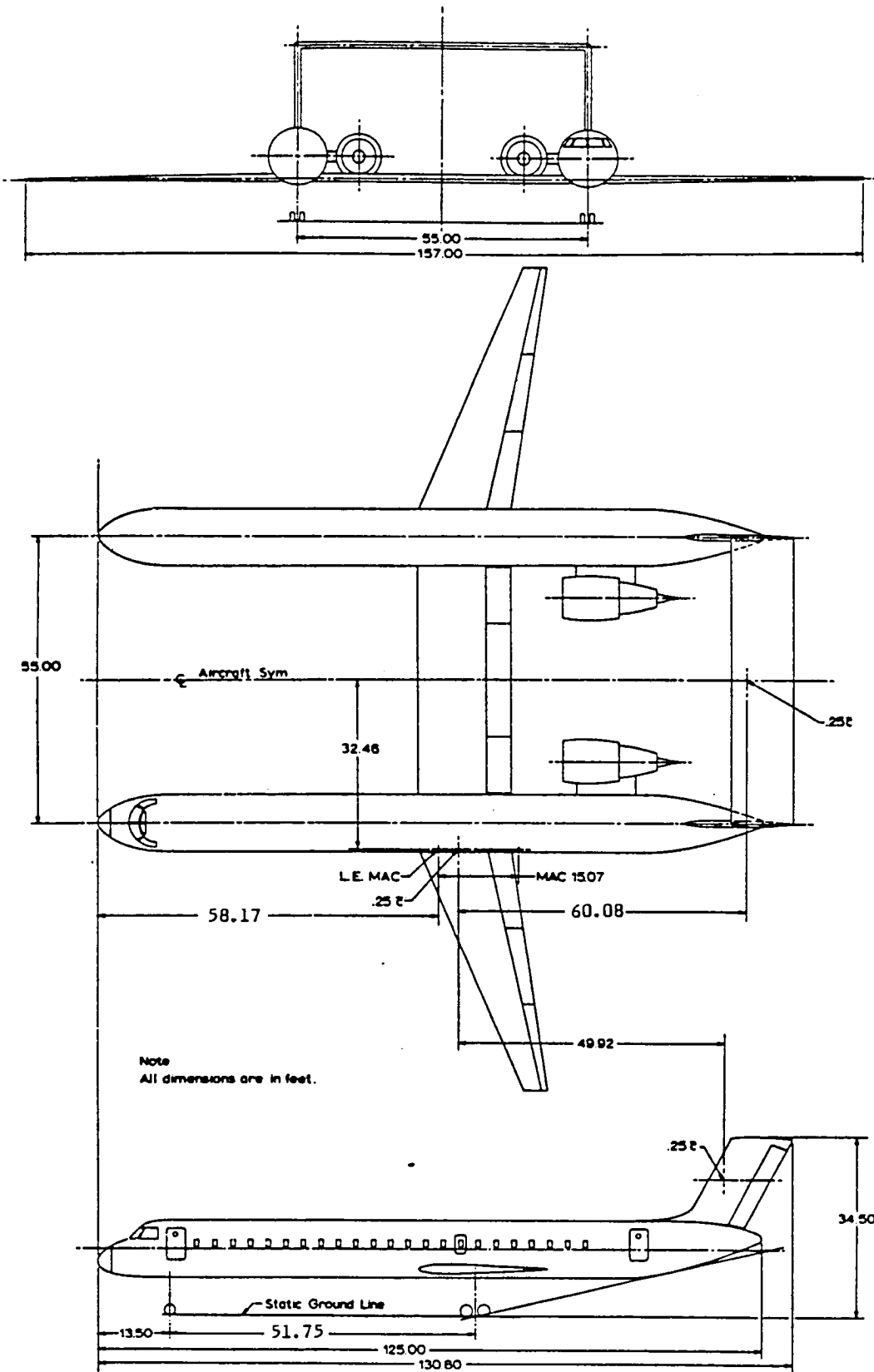
The following sections describe the experiment design, mechanization, and results from this study.

Section 2 EXPERIMENT DESIGN

2.1 AIRCRAFT MODEL

The baseline twin-fuselage aircraft was a 250 passenger transport design with the cockpit located in the nose of the left fuselage (Figure 1). The important physical characteristics are shown in Table 1 along with the trim conditions for the simulation. The linear non-dimensional stability and control derivatives are shown in Table 2. The only non-linear characteristics were the C_D and C_M versus α , and ground effect which are shown in Table 3 and 4.

Block diagrams of the longitudinal, roll, yaw, and autothrottle control systems are shown in Figures 2, 3, 4, and 5. The feel system and controller characteristics are shown in Table 5.



Twin Body Transport
4-7-82 ees

Figure 1 GENERAL TWIN-FUSELAGE TRANSPORT ARRANGEMENT

Table 1
TWIN FUSELAGE PHYSICAL CHARACTERISTICS
AND TRIM CONDITIONS

Weight = 193,000 lb

$I_{xx} = 4,003,900 \text{ slug-ft}^2$

$I_{yy} = 5,408,550 \text{ slug-ft}^2$

$I_{zz} = 9,181,470 \text{ slug-ft}^2$

$I_{xz} = 223,410 \text{ slug-ft}^2$

$S = 2147 \text{ ft}^2$

$\bar{c} = 15.074 \text{ ft}$

$b = 157 \text{ ft}$

$CG = 0.62 \bar{c}$

Landing Gear - down

$\gamma = 0^\circ$

$h = 2000 \text{ ft}$

$V = 132 \text{ kt}$

Flap = 50°

$\alpha_{Trim} = 3.15^\circ$

$\delta_{h_{Trim}} = -6.96^\circ$

$\delta_{e_{Trim}} = 0^\circ$

Thrust = 30,620 lb

Pilot eye relative to CG @ $0.62 \bar{c}$

$X_{pMCG} = 58.5 \text{ ft}$

$Y_{pMCG} = -29.13 \text{ ft (variable)}$

$Z_{pMCG} = -3.69 \text{ ft}$

Table 2
TWIN FUSELAGE NON-DIMENSIONAL
STABILITY AND CONTROL DERIVATIVES

C_{L_0} , 1/deg	1.1499	C_{y_β} , 1/deg	-.03136
C_{L_α} , 1/deg	.1144	C_{y_p} , 1/deg	.00563
$C_{L_{\delta_e}}$, 1/deg	.0149	C_{y_r} , 1/deg	.01345
$C_{L_{LG}}$	0	$C_{y_{\delta_a}}$, 1/deg	0
$C_{L_{GE}}$.0920F(h)	$C_{y_{\delta_{SP}}}$, 1/deg	0
$C_D(\alpha)$	Table 3	$C_{y_{\delta_r}}$, 1/deg	.00536
$C_{D_{\delta_e}}$, 1/deg	.00005	C_{l_β} , 1/deg	-.00256
$C_{D_{LG}}$.01493	C_{l_p} , 1/deg	-.01022
$C_{D_{GE}}$	-.0928F(h)	C_{l_r} , 1/deg	.00749
$C_m(\alpha)$	Table 3	$C_{l_{\delta_a}}$, 1/deg	.00148
$C_{m_{\delta_e}}$, 1/deg	-.0443	$C_{l_{\delta_{SP}}}$, 1/deg	.00023
$C_{m_{\delta_h}}$, 1/deg	-.0642	$C_{l_{\delta_r}}$, 1/deg	.00050
$C_{m_{LG}}$	-.0087	C_{n_β} , 1/deg	.00394
$C_{m_{GE}}$	-.0072F(h)	C_{n_p} , 1/deg	-.00074
C_{m_α} , 1/deg	-.1352	C_{n_r} , 1/deg	-.00552
C_{m_q} , 1/deg	-.5848	$C_{n_{\delta_a}}$, 1/deg	.00023
		$C_{n_{\delta_{SP}}}$, 1/deg	.00024
		$C_{n_{\delta_r}}$, 1/deg	-.00169

Table 3
NON LINEAR $C_D(\alpha)$ AND $C_m(\alpha)$

α , Deg	$C_D(\alpha)$	$C_m(\alpha)$
-8	.12603	-.0430
-4	.13883	-.2215
0	.17553	-.3703
4	.24753	-.4405
8	.35503	-.4638
12	.46453	-.4587

Table 4
GROUND EFFECT

h_{WH} , FT	$F_L(h)$ and $F_m(h)$	$F_D(h)$
157	0	0
130	.002	.011
110	.006	.033
90	.013	.070
80	.021	.097
70	.034	.131
60	.054	.174
50	.085	.227
40	.128	.294
30	.188	.391
20	.275	.519
10	.435	.714
0	1.000	1.000

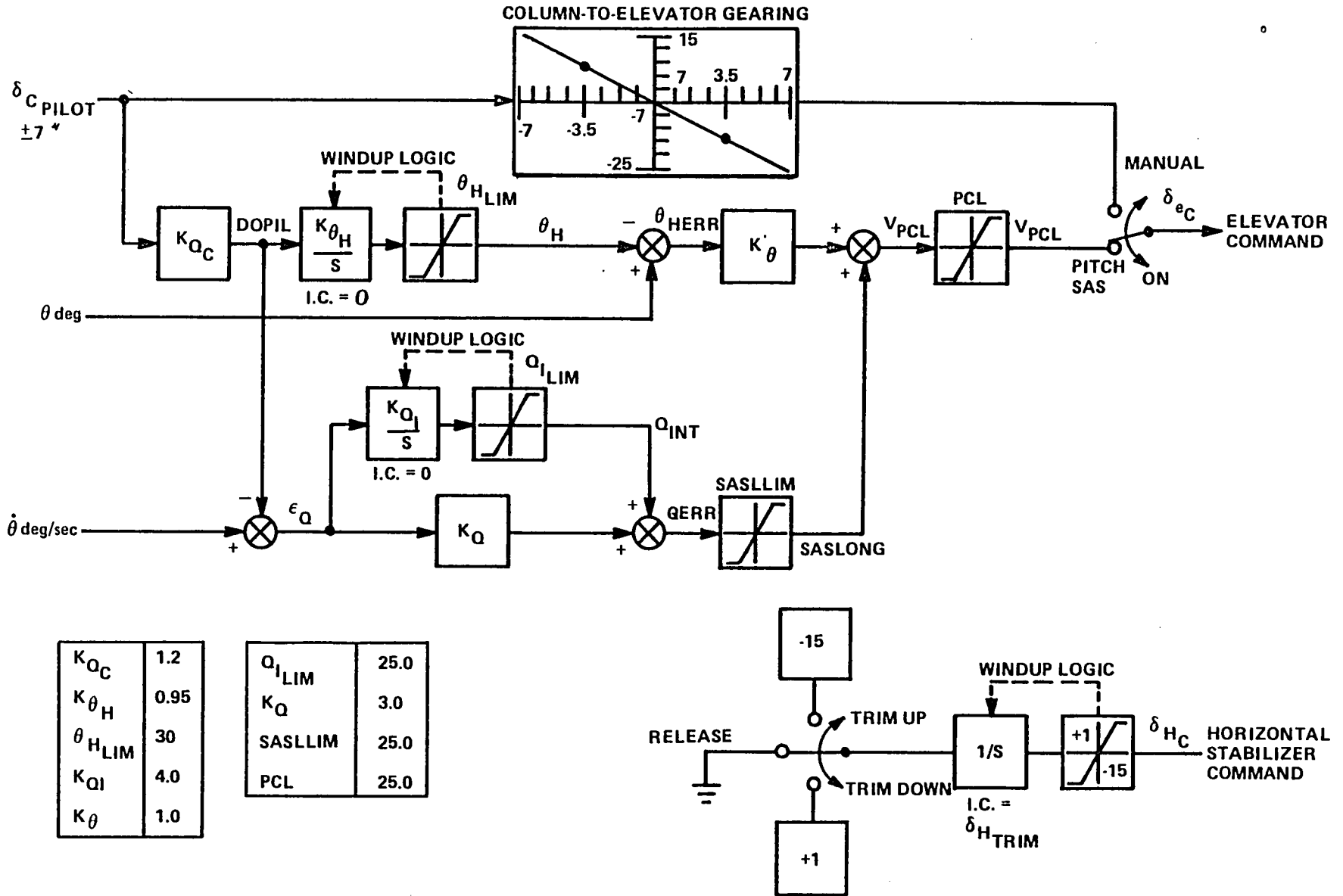


Figure 2 LONGITUDINAL CONTROL SYSTEM

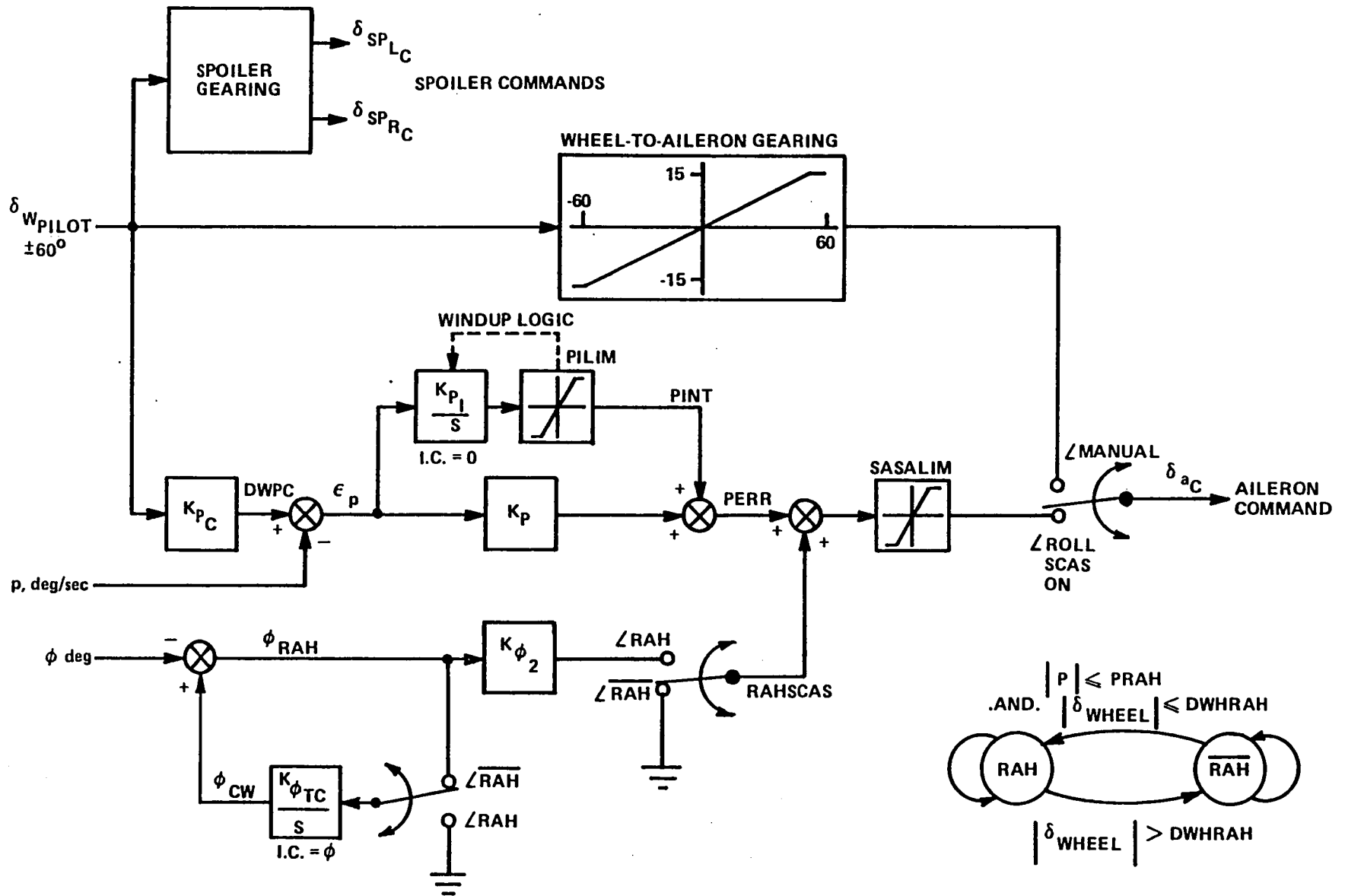


Figure 3 ROLL CONTROL SYSTEM

	SCAS		
	1	2	3
K_{PC}	.37	.40	.60
K_P	5.0	2.0	1.0
K_{PI}	4.95	2.0	1.0
K_{ϕ_2}	0	10.0	0

$K_{\phi_{TC}}$	-50
K_{WL}	1.0
PRAH	1.0
DWHRAH	0.3
PILIM	15.0
SASALIM	15.0

$$DW = \delta_{WPILOT} * \frac{113}{60}$$

$$\delta_{SP_{LC}} = \begin{cases} 0, & \delta_{WPILOT} > 0. \\ DSPFO, & \delta_{WPILOT} \leq 0. \end{cases}$$

$$\delta_{SP_{RC}} = \begin{cases} DSPFO, & \delta_{WPILOT} > 0. \\ 0, & \delta_{WPILOT} \leq 0. \end{cases}$$

$$\delta_{SP} = \delta_{SP_R} - \delta_{SP_L}$$

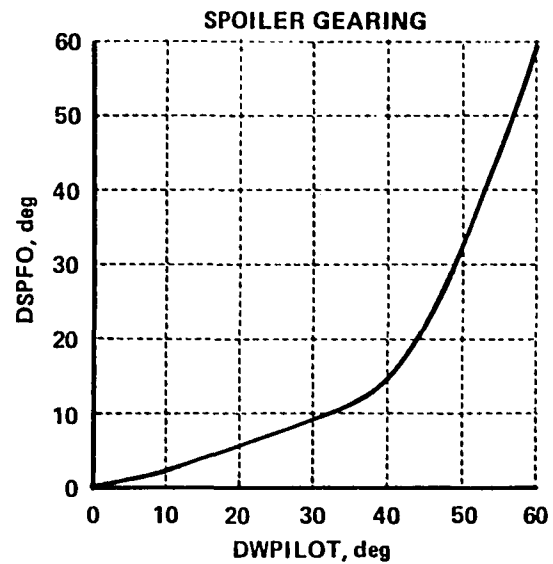


Figure 3 ROLL CONTROL SYSTEM (Cont.)

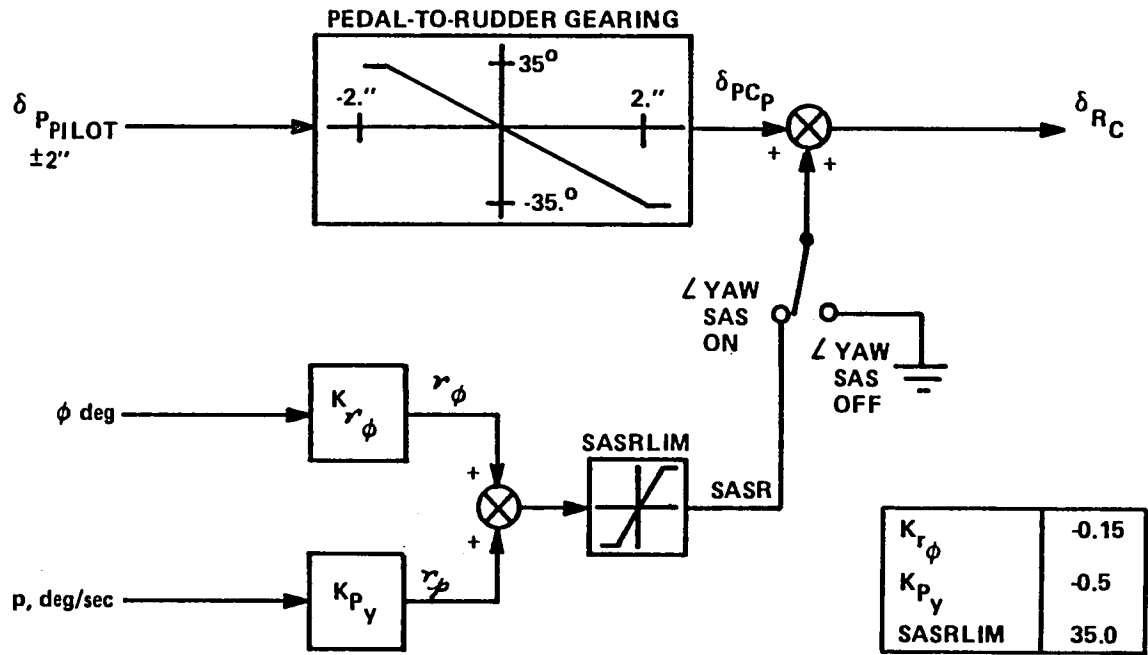
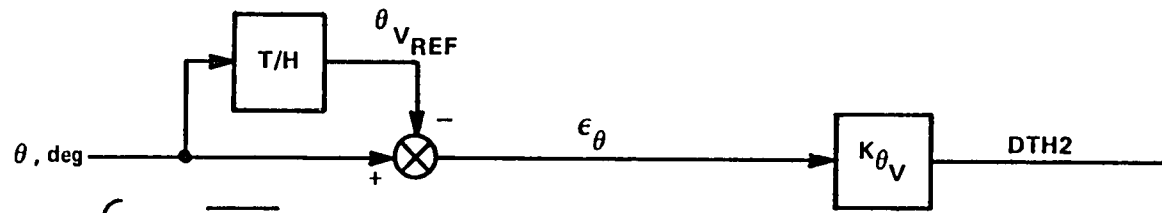
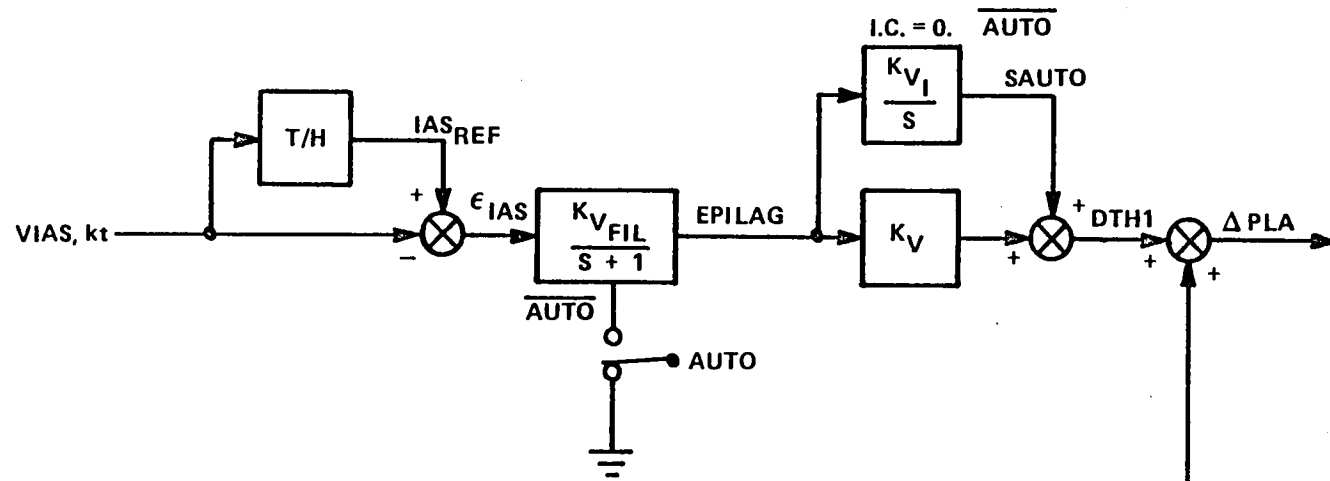


Figure 4 YAW CONTROL SYSTEM

2-10



T/H = $\begin{cases} \text{TRACK, } \overline{\text{AUTO}} \\ \text{HOLD, AUTO} \end{cases}$

$K_{V_{FIL}}$	0.518
K_{V_I}	0.14
K_V	3.9
K_{θ_V}	2.5

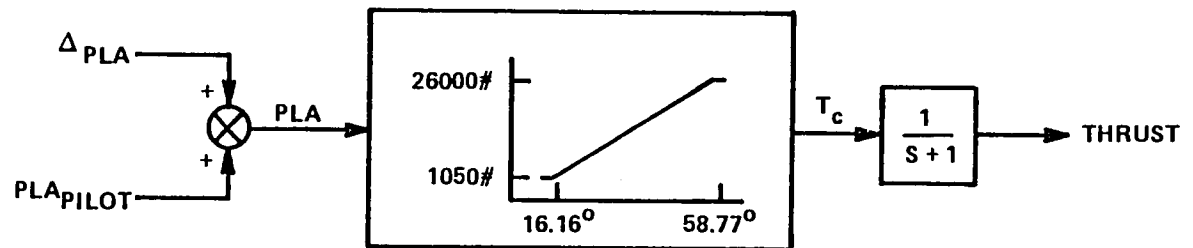


Figure 5 AUTO THROTTLE

Table 5
FEEL SYSTEM AND CONTROLLER CHARACTERISTICS

FUNCTION	UNITS	COLUMN	WHEEL	RUDDER
Beep Rate	deg/sec	-	21.4	-
Inertia	slug-ft ²	1.3	0.66	1.72
Viscous Friction	$\frac{\text{ft-lbf}}{\text{rad/sec}}$	12.3	4.4	23.6
Deadband	deg	-	1.0	-
Cable Stretch	%	0	0	0
Breakout (Pos)	lbfs	5.0 (Aft)	2.0 (R)	12.0 (R)
Breakout (Neg)	lbfs	3.0 (Fwd)	2.0 (L)	12.0 (L)
Static Friction	ft-lbf	0	0	1.1
Position Limit (Pos)		7.0 in (Aft)	60. deg (R)	2.0 in (R)
Position Limit (Neg)		7.0 in (Fwd)	60. deg (L)	2.0 in (L)
Spring Gradient		6.0 lbf/in	0.27 lbf/°	35.6 lbf/in
Frequency f_n	Hertz	3.3	0.56	1.88
Damping Ratio		0.23	0.96	0.58

SURFACE	SYMBOL	LIMITS		SERVO TIME CONSTANT
		DEFLECTION	RATE	
PITCH CONTROL Horizontal Tail	δ_h	+1 to -15°	1/3°/sec	-
Elevator	δ_e	+15° to -25°	25°/sec	0.1 sec
ROLL CONTROL Aileron	δ_a	±15°	15°/sec	0.1 sec
Spoiler	δ_{sp}	0 to 60°	60°/sec	-
YAW CONTROL Rudder	δ_r	±35°	25°/sec	0.1 sec

The equations of motion programed into the TIFS digital computer were
(subscript M refers to a model parameter)

Force Equations (in degrees)

$$1. \quad \dot{V}_M = \frac{-\bar{q}S}{m} (C_D \cos \beta_M - C_Y \sin \beta_M) - g \sin \gamma_M \\ + \frac{T}{m} \cos \alpha_M \cos \beta_M$$

$$\text{where: } \sin \gamma_M = \cos \beta_M (\cos \alpha_M \sin \theta - \sin \alpha_M \cos \theta \cos \phi) \\ - \sin \beta_M \cos \theta \sin \phi$$

$$2. \quad \dot{\alpha}_M = \frac{-57.3 \bar{q}S C_L}{m V_M \cos \beta_M} + \frac{57.3 g}{V_M \cos \beta_M} (\cos \theta_M \cos \phi_M \cos \alpha_M + \sin \theta_M \sin \alpha_M) \\ + q_M - \tan \beta_M (p_M \cos \alpha_M + r_M \sin \alpha_M) \\ - T \sin \alpha_M \frac{57.3}{m V_M \cos \beta_M}$$

$$3. \quad \dot{\beta}_M = \frac{57.3 \bar{q}S}{m V_M} (C_Y \cos \beta_M + C_D \sin \beta_M) \\ + \frac{57.3 g}{V_M} [\cos \theta_M \cos \beta_M \sin \phi_M - \sin \beta_M (\cos \theta_M \cos \phi_M \sin \alpha_M - \sin \theta_M \cos \alpha_M)] \\ + p_M \sin \alpha_M - r_M \cos \alpha_M \\ - T \cos \alpha_M \sin \beta_M \frac{57.3}{m V_M}$$

Note: T - thrust, assumed to act along x-body axis through CG

\bar{q} - dynamic pressure, $\frac{1}{2} \rho V^2$

Moment Equations (body axis)

$$4. \quad \dot{q}_M = \frac{57.3 \bar{q} S \bar{c}}{I_{yy}} C_m + \frac{I_{zz} - I_{xx}}{I_{yy}} \frac{p_M r_M}{57.3} + \frac{I_{xz}}{I_{yy}} \frac{r_M^2 - p_M^2}{57.3}$$

$$5. \quad \dot{p}_M = \frac{(57.3) \bar{q} S b}{I_{xx}} C_l + \frac{I_{yy} - I_{zz}}{I_{xx}} \frac{q_M r_M}{57.3} + \frac{I_{xz}}{I_{xx}} \left(\dot{r}_M + \frac{p_M - q_M}{57.3} \right)$$

$$6. \quad \dot{r}_M = \frac{(57.3) \bar{q} S b}{I_{zz}} C_n + \frac{I_{xx} - I_{yy}}{I_{zz}} \frac{q_M p_M}{57.3} + \frac{I_{xz}}{I_{zz}} \left(\dot{p}_M + \frac{q_M - r_M}{57.3} \right)$$

Nondimensional aerodynamic coefficients were defined by the following equations:

$$a. \quad C_D = C_D(\alpha) + C_{D_{\delta_e}} \delta_e + C_{D_{LG}}(LG) + C_{D_{GE}} F_D(h)$$

$$b. \quad C_L = C_{L_0} + C_{L_\alpha} \alpha + \frac{\bar{c}}{2V} (C_{L_{\dot{\alpha}}} \dot{\alpha} + C_{L_q} q) + C_{L_{\delta_e}} \delta_e + C_{L_{LG}}(LG) + C_{L_{GE}} F_L(h)$$

$$\begin{aligned}
 \text{c. } C_m &= C_m(\alpha) + \frac{\bar{c}}{2V} (C_{m_\alpha} \dot{\alpha} + C_{m_q}) \\
 &\quad + C_{m_{\delta_e}} \delta_e + C_{m_{\delta_H}} \delta_H + C_{m_{LG}} (LG) + C_{m_{GE}} F_m(h)
 \end{aligned}$$

$$\begin{aligned}
 \text{d. } C_n &= C_{n_\beta} \beta + C_{n_{\delta_r}} \delta_r + \frac{b}{2V} (C_{n_p} p + C_{n_r} r) \\
 &\quad + C_{n_{\delta_a}} \delta_a + C_{n_{\delta_{SP}}} \delta_{SP}
 \end{aligned}$$

$$\begin{aligned}
 \text{e. } C_l &= \frac{b}{2V} (C_{l_p} p + C_{l_r} r) + C_{l_\beta} \beta + C_{l_{\delta_a}} \delta_a + C_{l_{\delta_{SP}}} \delta_{SP} \\
 &\quad + C_{l_{\delta_r}} \delta_r
 \end{aligned}$$

$$\begin{aligned}
 \text{f. } C_y &= C_{y_\beta} \beta + C_{y_{\delta_a}} \delta_a + C_{y_{\delta_{SP}}} \delta_{SP} + C_{y_{\delta_r}} \delta_r \\
 &\quad + \frac{b}{2V} (C_{y_p} p + C_{y_r} r)
 \end{aligned}$$

2.2 CONFIGURATIONS

Variations in the acceleration environment and flying qualities from the baseline aircraft were obtained by changes in the location of the pilot position off of the centerline and changes in the effective roll mode constant. Three pilot positions were chosen: $y_p = 0$ ft, 30 ft (actually the baseline was 29.13 ft), and 50 ft. The off-centerline pilot positions were to the left of centerline. The variations in roll mode time constant were obtained by changing the K_{pC} , K_p , and K_{pI} gains in the lateral control system, they are identified on Figure 3. The effective roll mode time constants were measured from the roll rate response to a step input by taking the time to reach 63% of steady state. The measured roll mode time constants are:

SCAS - 1	$\tau_R = .6$ sec
SCAS - 2	$\tau_R = 1.2$ sec
SCAS - 3	$\tau_R = 2.3$ sec

Time histories of step inputs into the pitch axis (same for all configurations) and roll axis for each configuration are shown in Figures 6, 7, 8, and 9. Only pitch rate, roll rate, and normal acceleration at the pilot position are shown. The effective roll mode time constants are noted for each configuration. Note the level of normal acceleration achieved with the various pilot positions and roll mode time constants.

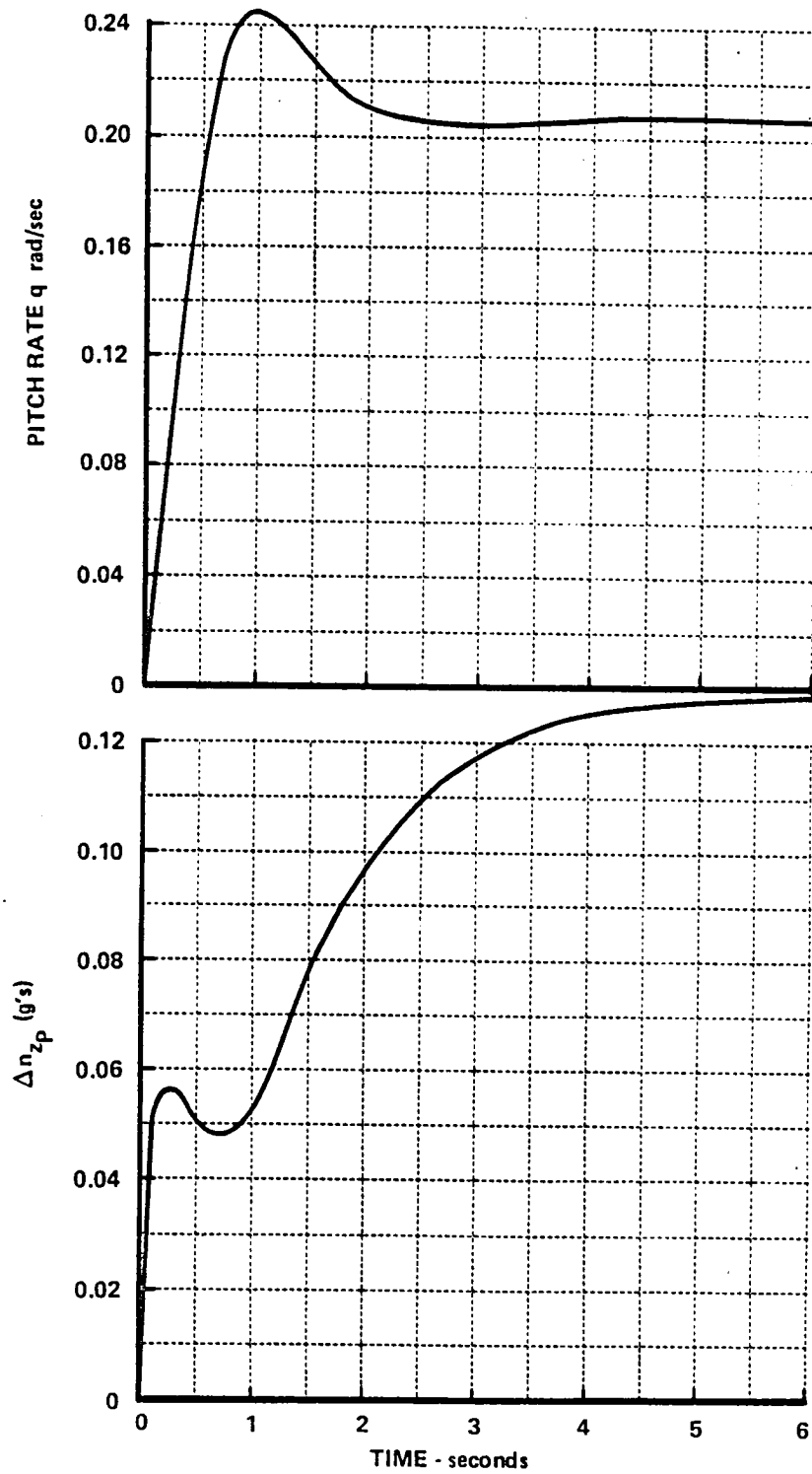


Figure 6 PITCH RATE AND N_{z_p} RESPONSE TO STEP INPUT

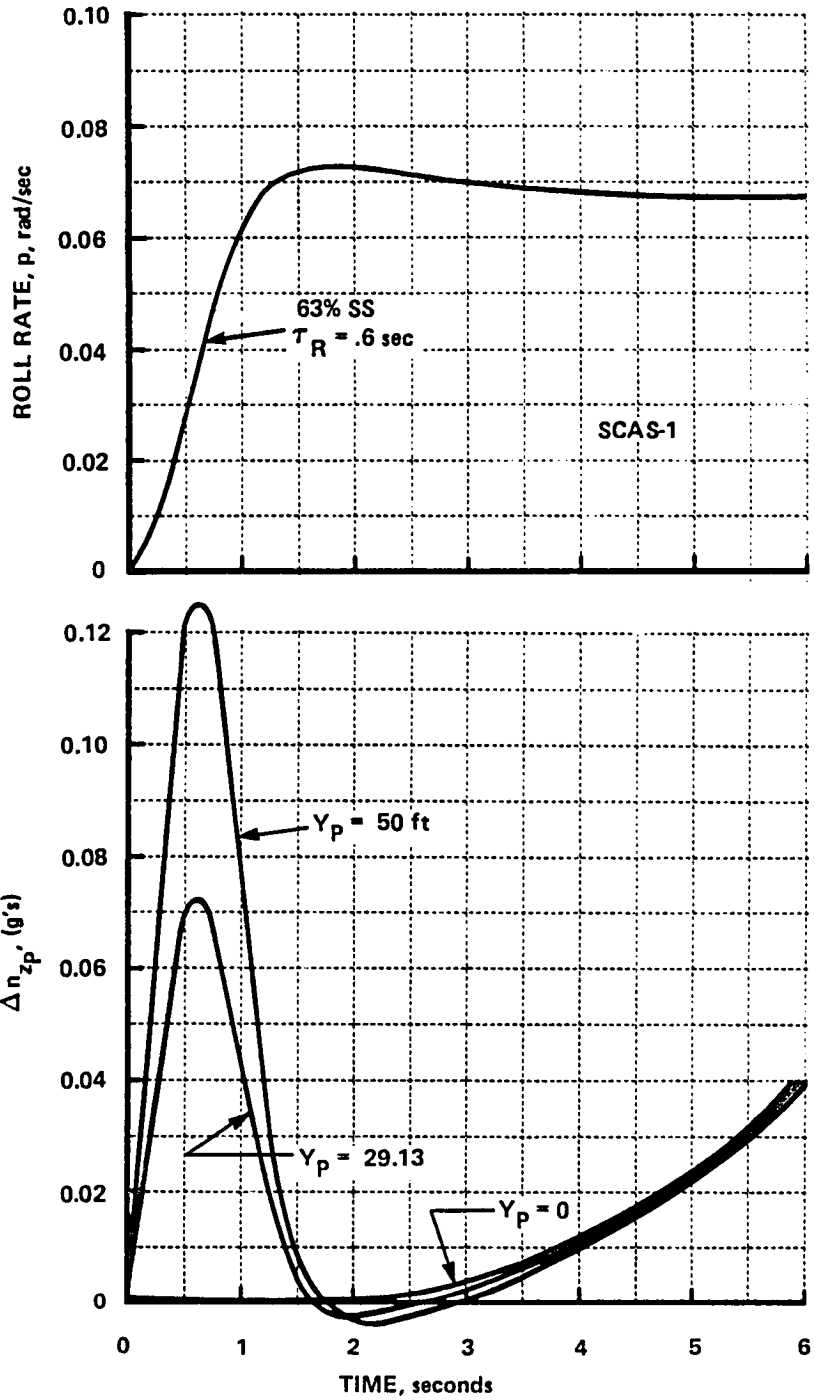


Figure 7 ROLL RATE AND N_{z_p} RESPONSE TO STEP INPUT, SCAS-1

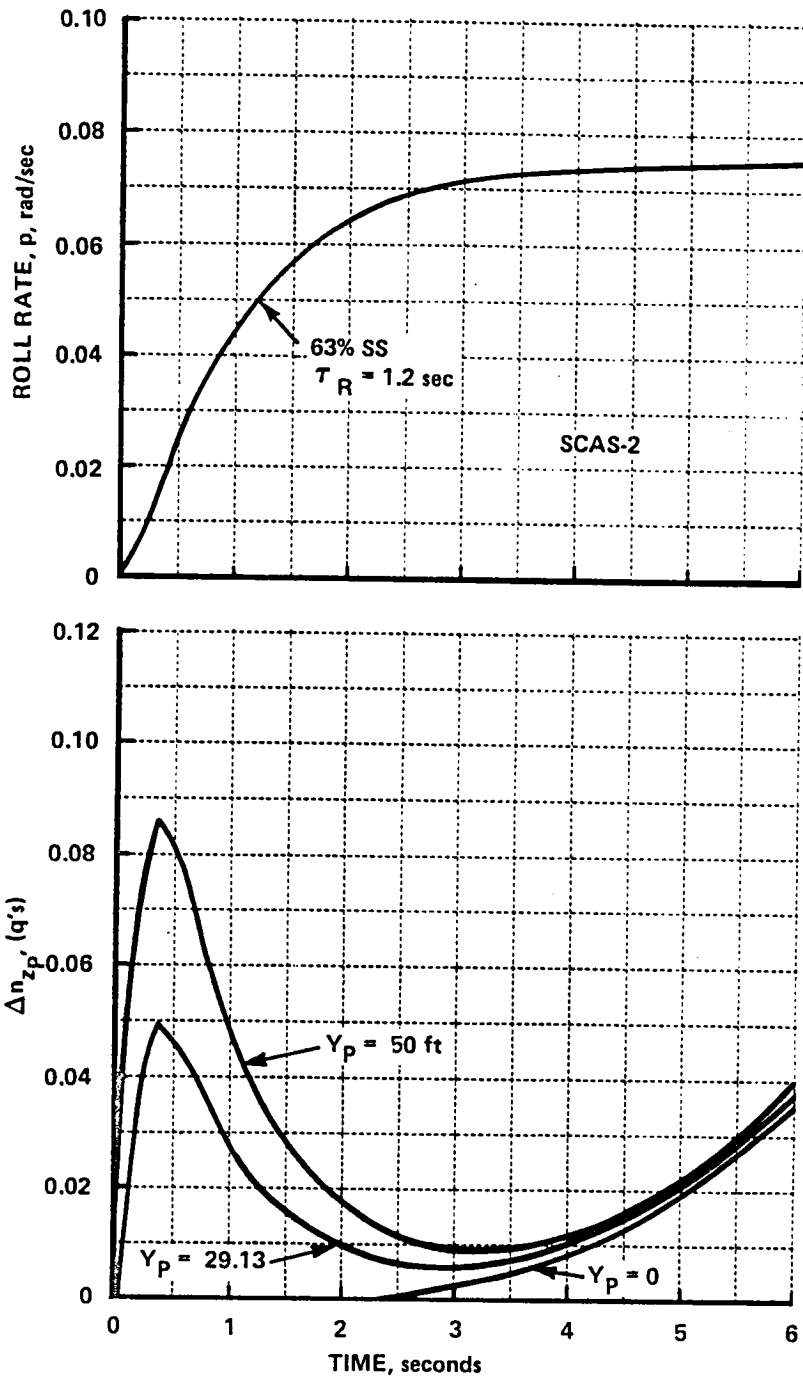


Figure 8 ROLL RATE AND N_{z_p} RESPONSE TO STEP INPUT, SCAS-2

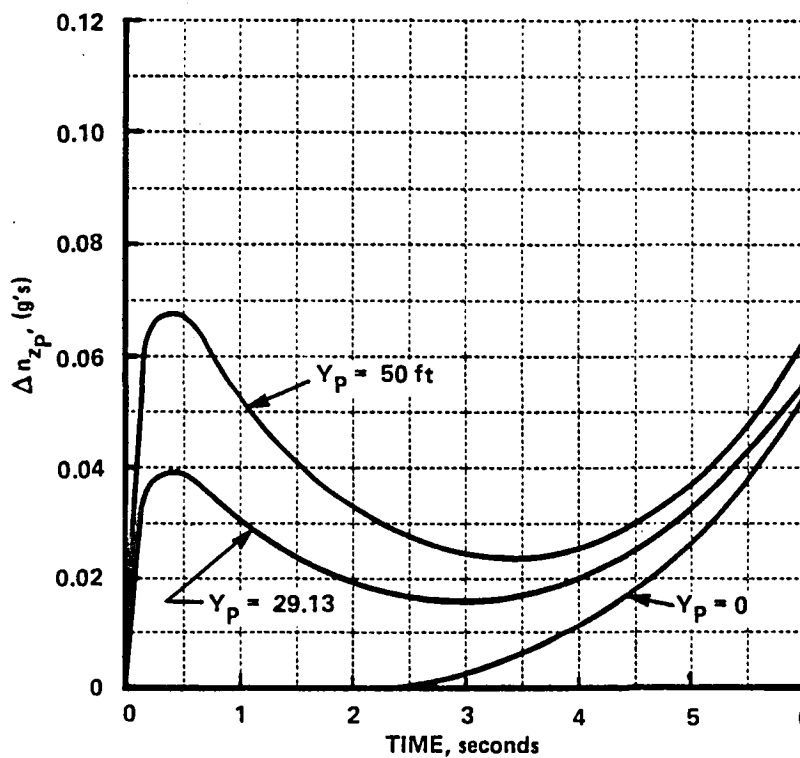
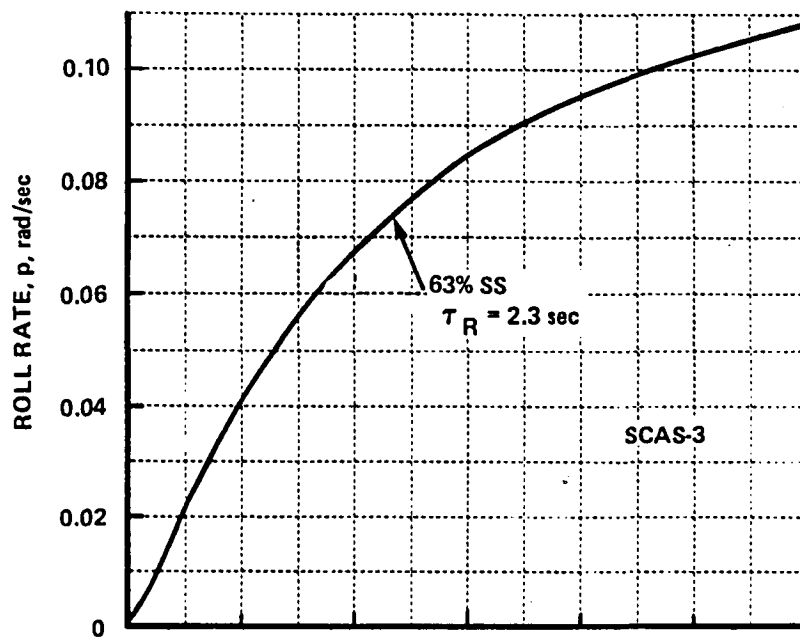


Figure 9 ROLL RATE AND N_z RESPONSE TO STEP INPUT, SCAS-3

The flying qualities of the baseline aircraft were all generally Level 1. A listing of the important flying qualities parameters are shown in Table 6.

Table 6
FLYING QUALITIES CHARACTERISTICS

ω_{SP}	=	2.7 rad/sec
ξ_{SP}	=	.69
n_z/α	=	4.32 g/rad
ω_{ph}	=	.26 rad/sec
ξ_{ph}	=	1.2
τ_R	=	.6 sec (SCAS - 1)
		1.2 sec (SCAS - 2)
		2.3 sec (SCAS - 3)
ω_D	=	.77 rad/sec
ξ_D	=	.30
$ \phi/\beta $	=	.2
ω_ϕ/ω_D	=	1.0
ξ_ϕ/ξ_D	=	1.0

2.3 TEST DESCRIPTION

2.3.1 Introduction

A test matrix consisting of nine separate configurations made up of the three pilot positions with the three roll mode time constants was generated. Two evaluation pilots each flew most of these configurations in an approach and landing task with lateral runway offsets, crosswinds, and natural turbulence added as environmental factors to increase the pilot workload. Pilot Comments and Cooper-Harper pilot ratings were given after each approach.

2.3.2 Evaluation Tasks and Procedures

The evaluation pilot was given control of the aircraft on the downwind leg at 1700 to 1800 ft AGL and performed a visual turning approach to a 1.5 to 2 mile final approach. The ILS glide slope was intercepted in the turn and was held until flare. A constant speed of 132 knots was held throughout the approach until landing flare. Artificial crosswinds of 15 knots (using the TIFS sideforce surfaces to set up a β mismatch) and a lateral offset of 200 ft (visually set up by the pilot) were used to provide secondary tasking, thus preventing pre-occupation with the pitch task and in order to force lateral corrections near touchdown. A combination of a right crosswind and a left lateral offset or left crosswind and right lateral offset was generally used as these combinations required the largest roll maneuvers and resulting normal accelerations at the pilot station. The lateral offset was held by the pilot to approximately one mile out at about 250 ft of altitude. The pilot then corrected to the runway centerline (pilot on runway centerline, regardless of where he was in the model aircraft). At 100 ft the autothrottle was disengaged in order to allow the speed to bleed off in the flare. From 50 ft on down the pilot attempted to decrab and bank the aircraft to make a wing low steady heading sideslip landing. A "desired" touchdown area was defined as being 500 ft long and 20 ft wide (± 10 ft off centerline) starting 250 ft past the runway/glide slope intercept. The "adequate" touchdown area was defined as 1000 ft long, 40 ft wide and starting at the same point on the runway. Airspeed requirements were: "desired" 132 ± 3 kt, "adequate" 132 ± 5 kt. "Desired" sink rate at touchdown was defined as 0 to 3 ft/s and "adequate" as 3 to 6 ft/s.

At touchdown the TIFS safety pilot would take control of the aircraft (or at any time prior to touchdown if dictated by the situation). At this point the evaluation pilot would give his comments and pilot ratings on the voice recorder and the TIFS test engineers would set up for the next approach. Due to maximum landing weight limitations, landings performed early in the flight could not be completed to actual touchdowns. For these approaches the safety pilot would take control at approximately 5 to 10 feet off the ground. On these approaches the pilot ratings dealing with the final touchdown phase were not given as the pilot's gain and aggressiveness were not as high as when actual touchdowns were made.

2.3.3 Pilot Comment Card and Rating Scale

The evaluation pilots were briefed on the general experiment purposes and flight task details. They had knowledge of experiment variables of pilot position and roll mode time constants. However, before each approach they were only told what the lateral pilot position was and not the SCAS configuration. This was done to allow the pilots to develop and use any different control techniques that may be required with an offset position and make him aware that unnatural vertical motions may occur with roll inputs.

The evaluation pilot could make comments at any time during the approach. However, formal pilot comments using comment card of Figure 10 as guide were given at the end of each approach. Cooper-Harper pilot ratings using the scale of Figure 11 were also given for each run. One rating was given for the approach portion only and one rating was given for the overall task including touchdown. For approaches which did not go to an actual touchdown only the approach rating was given. For some approaches which resulted in a pilot induced oscillation (PIO) a PIO rating using the PIO scale of Figure 12 was given.

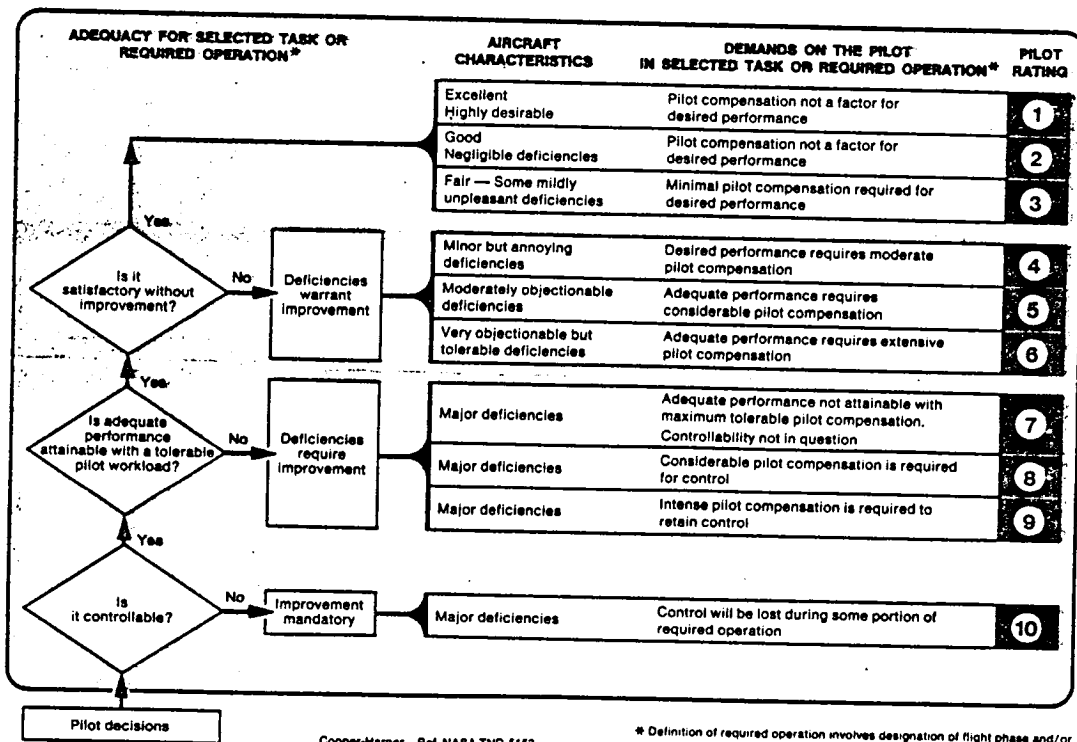
2.3.4 Evaluation Pilots

Two evaluation pilots participated in this flight program. They were NASA/Langley test pilots, Kenneth R. Yenni and AF Major William R. Neely (currently assigned to NASA/LRC). Both of these pilots have had extensive experience in flying qualities investigations and had participated in a previous ground simulator experiment dealing with twin-fuselage flying qualities. In the remainder of this report Major Neely and Mr. Yenni are referred to as Pilots A and B, respectively.

1. Feel
 - Column, wheel forces and displacements, harmony
 - Roll and pitch sensitivity
2. Response to inputs required to perform task
 - Roll and pitch
 - initial response
 - predictability of final response
 - pitch/roll harmony
 - special pilot inputs - why?
 - tendency to PIO
 - Linear acceleration
 - magnitude
 - influence on control technique
 - differences for right and left maneuvers
 - coordination in turns
3. Airspeed control - autothrottle OFF
4. Approach performance
 - ILS: glideslope, localizer capture and tracking
 - Visual: flight path corrections
5. Flare and touchdown
 - Problems with line-up flare, decrab, touchdown, tendency to float
 - Any unusual motions, visual cues, etc.
 - Any unusual control techniques required
6. Approach vs. landing
 - Which more difficult
7. Effects of turbulence/wind
8. Summary (brief)
 - Good features - Problems
9. Overall Cooper-Harper Rating - PIO Rating

Figure 10 PILOT COMMENT CARD

HANDLING QUALITIES RATING SCALE



Cooper-Harper Ref. NASA TND-5153

* Definition of required operation involves designation of flight phase and/or subphases with accompanying conditions.

- LEVEL 1 $PR \leq 3.5$
- LEVEL 2 $3.5 < PR \leq 6.5$
- LEVEL 3 $6.5 < PR \leq 9$

Figure 11 COOPER-HARPER HANDLING QUALITIES RATING SCALE

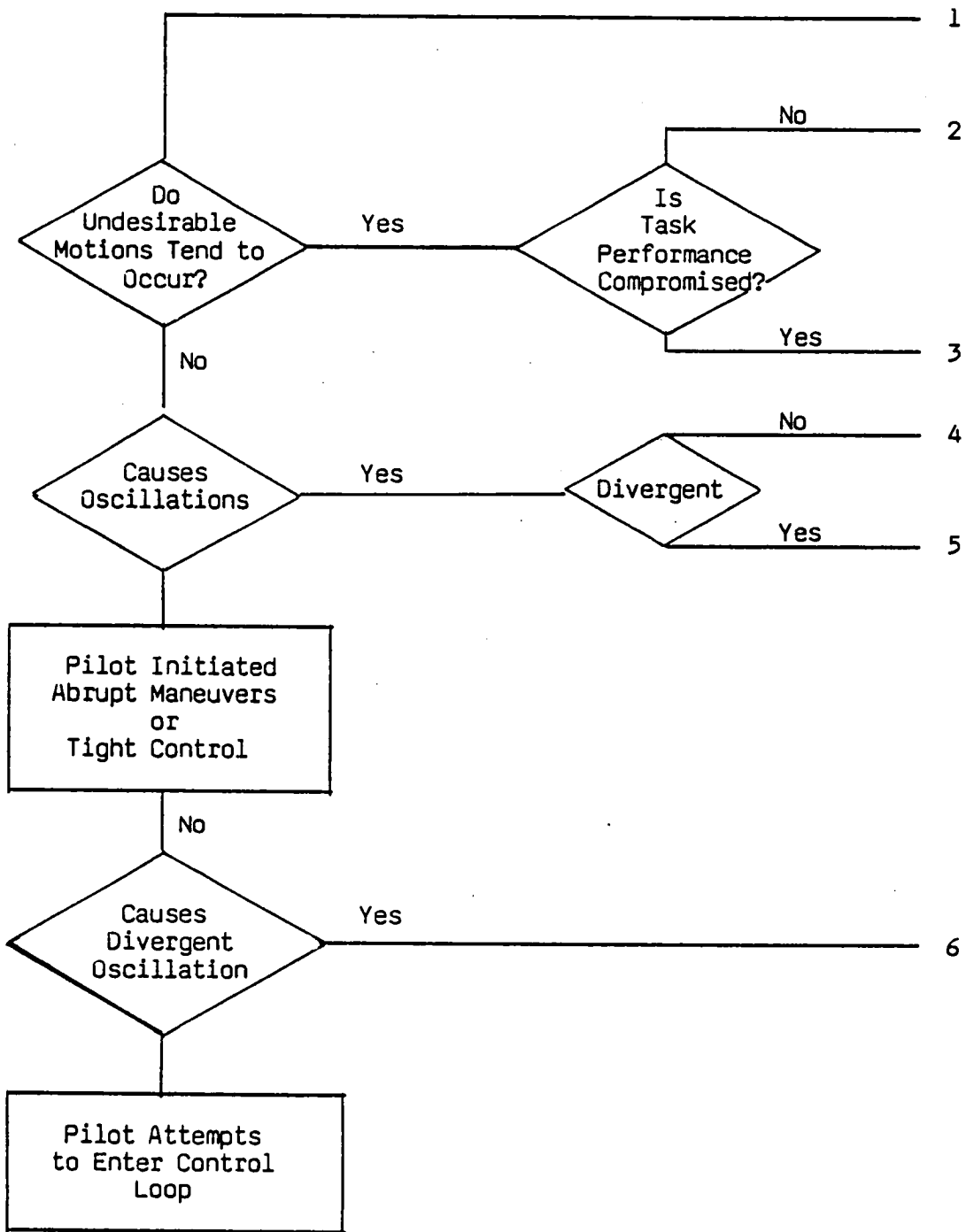


Figure 12 PIO TENDENCY CLASSIFICATION



Section 3 EXPERIMENT MECHANIZATION

3.1 EQUIPMENT

The USAF/AFWAL Total In-Flight Simulator (TIFS) was used as the test vehicle in this experiment. TIFS is a highly modified C-131 (Convair 580) configured as a six-degree-of-freedom simulator (Figure 13). It has a separate evaluation cockpit forward and below the normal C-131 cockpit. When flown from the evaluation cockpit in the simulation or fly-by-wire mode, the pilot control commands are fed as inputs to the model computer which calculates the aircraft response to be reproduced. These responses, along with TIFS motion sensor signals, are used to generate feedforward and response error signals, which drive the six controllers on the TIFS (Figure 14). The model-following system gains are documented in Appendix A. The result is a high fidelity reproduction of the motion and visual cues at the pilot position of the model aircraft. A detailed description of the TIFS can be found in Reference 3.

This experiment made use of the following major features inherent in the TIFS aircraft:

1. Independent control of all six forces and moments by use of elevator, aileron, rudder, throttle, direct lift flaps and side force surfaces.
2. Longitudinal and lateral/directional model-following systems to provide the evaluation pilot with motion and visual cues representative of the simulated aircraft.
3. Separate evaluation cockpit capable of accepting appropriate pilot controls and displays.
4. Evaluation cockpit instruments included standard IFR instrument displays featuring an ADI and an HSI as the primary instruments, with angle of attack displayed on an indicator on the right hand side of the HSI and

sideslip displayed on the indicator above the HSI. The vertical and horizontal bars on the ADI displayed command information for tracking localizer and glide slope, respectively.

5. Digital magnetic tape recording system to record control inputs and appropriate aircraft responses.
6. Two cassette tape voice recorders for recording evaluation pilot comments, and TIFS crew comments.
7. The capability to simulate artificial or cancel actual crosswinds up to 15 kts incorporated in the model-following system.
8. A signal light located above the ADI and audio signal to indicate touchdown of main landing gear.

The evaluation cockpit was configured as illustrated in Figure 15. The controls were standard wheel and rudders. Thrust was controlled by four throttle levers tied together and total thrust was indicated on a single gage. Asymmetric thrust control was not provided.

The evaluation pilot's instrument panel is shown in Figure 16. It was a standard configuration with flight director or raw data information available on the VSI.

TIFS evaluation cockpit is a dual pilot side by side arrangement. For this investigation the right seat was occupied by a NASA flight test engineer. The engineer observed all approaches and landings, assisted in conduct of the flight test card and recorded summarized evaluation pilot comments and handling qualities ratings to provide timely post flight analysis.

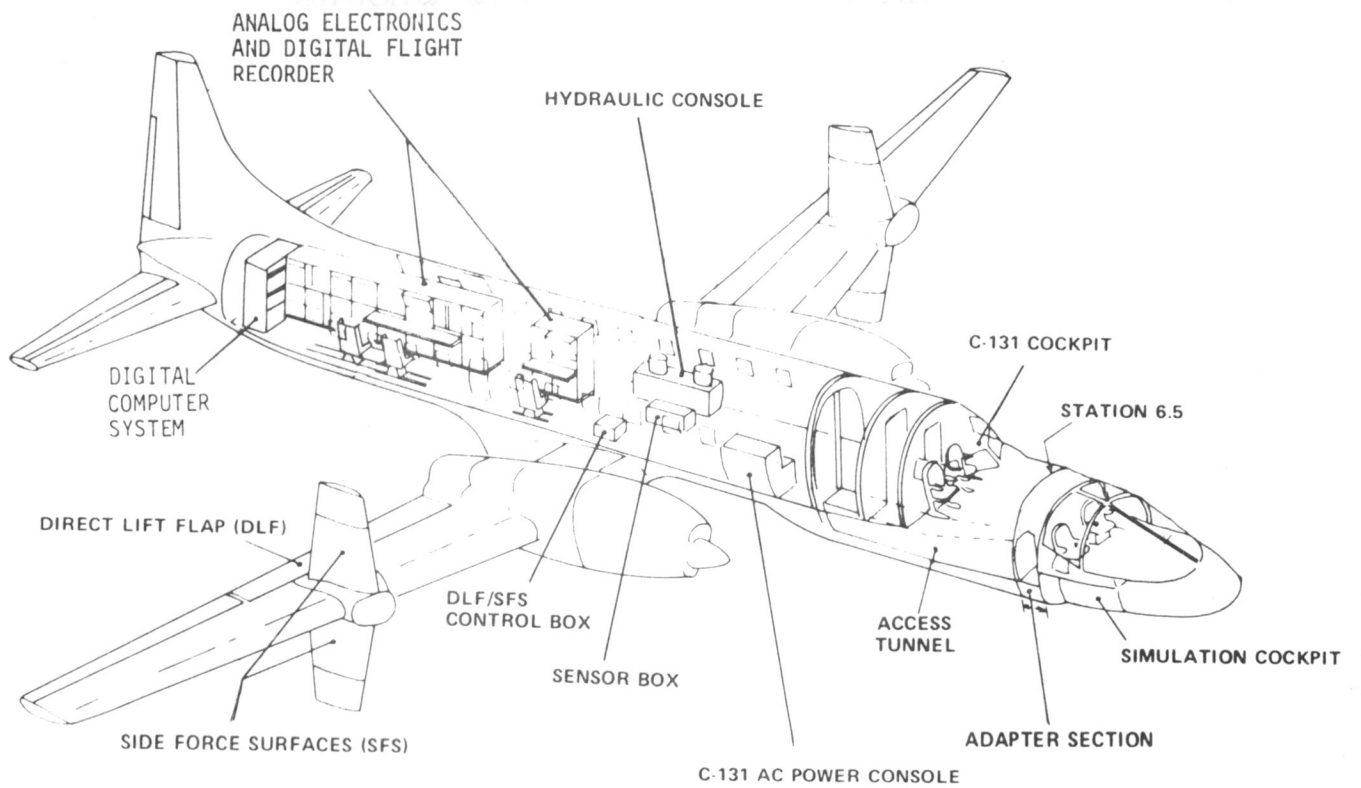
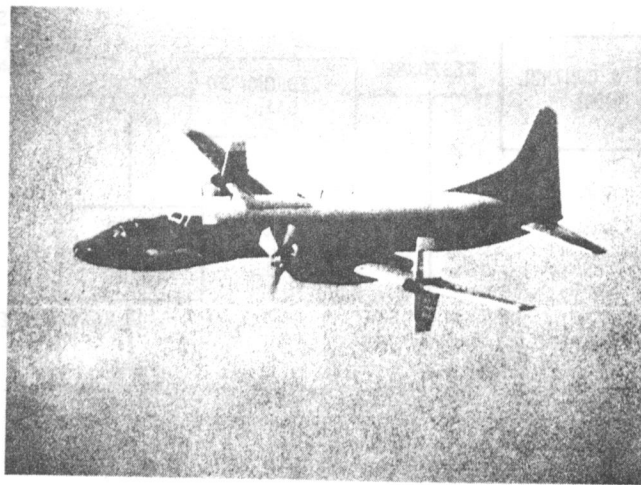


Figure 13 USAF/CALSPAN TOTAL IN-FLIGHT SIMULATOR (TIFS)

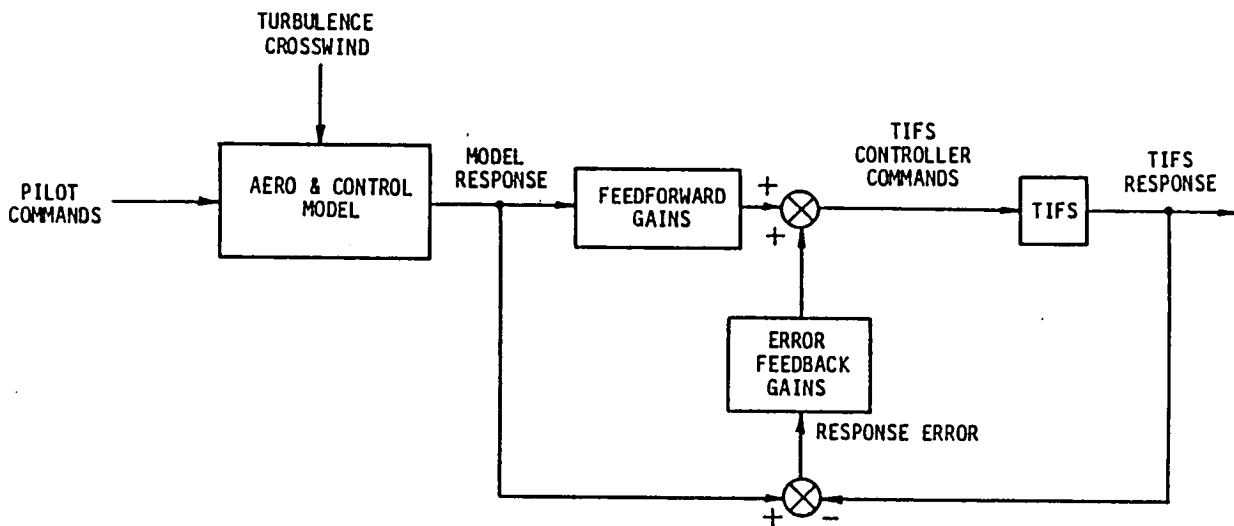


Figure 14 TIFS MODEL FOLLOWING SIMULATION



Figure 15 TIFS EVALUATION COCKPIT

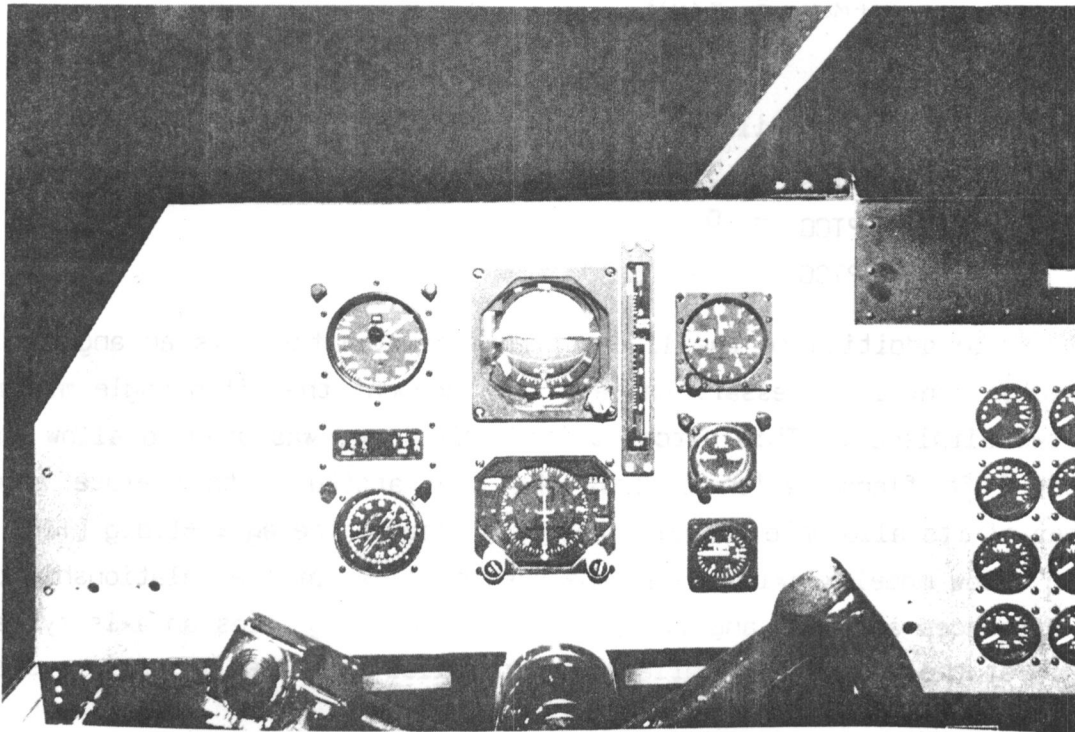


Figure 16 CAPTAIN'S INSTRUMENT PANEL IN EVALUATION COCKPIT

3.2 SIMULATION GEOMETRY AND TRANSFORMATION EQUATIONS

The TIFS motion simulation system was configured to reproduce the model's motion at the evaluation pilot's position. Since the distance between the CG of the TIFS and the evaluation pilot position is not the same as the CG to pilot position in the model (especially since the pilot may be offset 50 ft from the centerline) transformations of model states are necessary. These transform the appropriate model states from the model center of gravity to a point which corresponds to the TIFS CG when the pilot's eye positions coincide. We denote these transformed model variables with the subscript MF to signify that these are the motion variables which drive the model following system.

The distances of interest are (in feet):

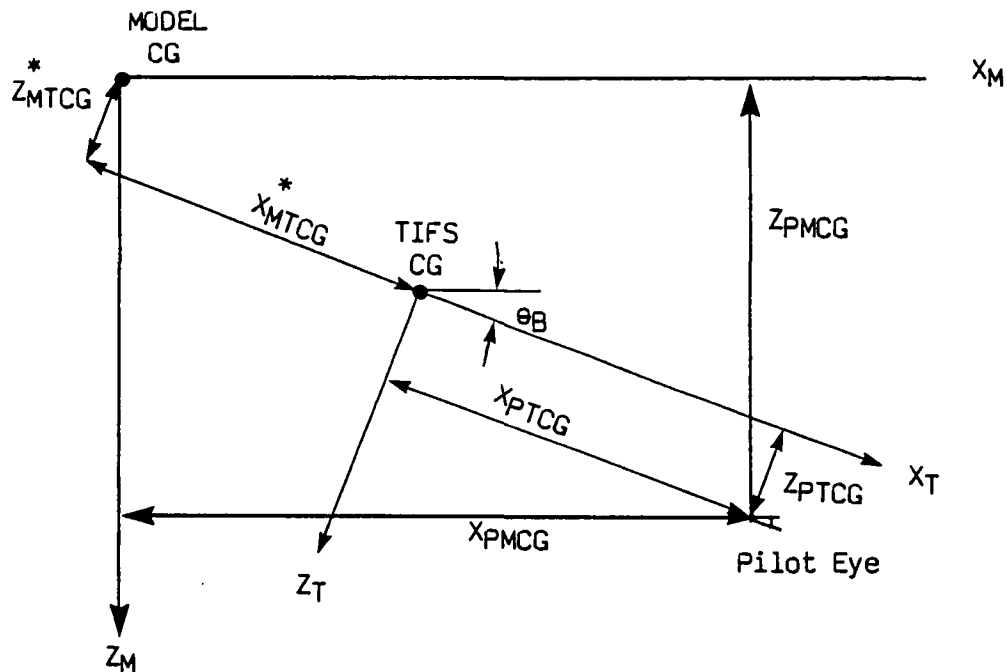
Twin-Fuselage - CG to Pilot:

$$\begin{aligned} X_{PMCG} &= 58.5 \\ Y_{PMCG} &= 0, -29.13, -50. (\text{for the three positions evaluated}) \\ Z_{PMCG} &= -3.69 \\ Y_p &= -Y_{PMCG} \end{aligned}$$

TIFS - CG to Pilot:

$$\begin{aligned} X_{PTCG} &= 33.8 \\ Y_{PTCG} &= 0 \\ Z_{PTCG} &= -1.5 \end{aligned}$$

In addition to the linear transformation there is an angular transformation that is necessary to take into account the pitch angle mismatch of the two airplanes. This pitch attitude bias, e_B , was used to allow the TIFS direct lift flaps, which control the trim attitude, to operate about the center of its allowable travel. For this program the $e_B = +1.\text{deg}$ (TIFS x-axis 1 deg below model x-axis). See the sketch below for the relationship between the distances and bias angle. The notation (*) signifies an axis system with origin at the model CG but orientation parallel with the TIFS axis system.



Therefore, the distances of interest from the model's CG to the TIFS CG in the TIFS body axes system are then:

$$X^*_{MTCG} = X_{PMCG} \cos \theta_B + Z_{PMCG} \sin \theta_B - X_{PTCG}$$

$$Y^*_{MTCG} = Y_{PMCG} - Y_{PTCG}$$

$$Z^*_{MTCG} = Z_{PMCG} \cos \theta_B - X_{PMCG} \sin \theta_B - Z_{PTCG}$$

$$X^*_{MTCG} = 58.5 \cos \theta_B - 3.69 \sin \theta_B - 33.8 = 24.6$$

$$Y^*_{MTCG} = 0, -29.13, -50.0 = 0, -29.13, -50.$$

$$Z^*_{MTCG} = -3.69 \cos \theta_B - 58.5 \sin \theta_B + 1.5 = -3.2$$

The following equations were then used in the model computer to define kinematics of the model in the appropriate axes systems (all angular units are degrees).

Model accelerations at its CG and in model body axes system:

$$n_X = \frac{\bar{q}S}{mg} (C_L \sin \alpha - C_D \cos \alpha) + \frac{T}{mg}$$

$$n_Y = \frac{\bar{q}S}{mg} (C_Y)$$

$$n_Z = -\frac{\bar{q}S}{mg} (C_L \cos \alpha + C_D \sin \alpha)$$

Model accelerations at pilot's station in model body axes system:

$$n_{X_p} = n_X + \frac{1}{57.3g} \left[-X_{PMCG} \left(\frac{r^2 + q^2}{57.3} \right) + Y_{PMCG} \left(\frac{pq}{57.3} - \dot{i} \right) + Z_{PMCG} \left(\frac{pr}{57.3} + \dot{q} \right) \right]$$

$$n_{Y_p} = n_Y + \frac{1}{57.3g} \left[X_{PMCG} \left(\frac{pq}{57.3} + \dot{i} \right) - Y_{PMCG} \left(\frac{p^2 + r^2}{57.3} \right) + Z_{PMCG} \left(\frac{qr}{57.3} - \dot{p} \right) \right]$$

$$n_{Z_p} = n_Z + \frac{1}{57.3g} \left[X_{PMCG} \left(\frac{pr}{57.3} - \dot{q} \right) + Y_{PMCG} \left(\frac{qr}{57.3} + \dot{p} \right) - Z_{PMCG} \left(\frac{q^2 + p^2}{57.3} \right) \right]$$

Model accelerations at its CG in TIFS body axes system:

$$n_X^* = n_X \cos \theta_B + n_Z \sin \theta_B$$

$$n_Y^* = n_Y$$

$$n_Z^* = n_Z \cos \theta_B - n_X \sin \theta_B$$

Model accelerations at pilot's station in TIFS body axes system:

$$n_{X_{MF}}^* = n_X^* + \frac{1}{57.3g} \left[-X_{PMCG}^* \left(\frac{r^{*2} + q^{*2}}{57.3} \right) + Y_{PMCG}^* \left(\frac{p^*q^*}{57.3} - \dot{i}^* \right) + Z_{PMCG}^* \left(\frac{p^*r^*}{57.3} + \dot{q}^* \right) \right]$$

$$n_{Y_{MF}}^* = n_Y^* + \frac{1}{57.3g} \left[X_{PMCG}^* \left(\frac{p^*q^*}{57.3} + \dot{i}^* \right) - Y_{PMCG}^* \left(\frac{p^{*2} + r^{*2}}{57.3} \right) + Z_{PMCG}^* \left(\frac{q^*r^*}{57.3} - \dot{p}^* \right) \right]$$

$$n_{Z_{MF}}^* = n_Z^* + \frac{1}{57.3g} \left[X_{PMCG}^* \left(\frac{p^*r^*}{57.3} - \dot{q}^* \right) + Y_{PMCG}^* \left(\frac{q^*r^*}{57.3} + \dot{p}^* \right) - Z_{PMCG}^* \left(\frac{r^{*2} + p^{*2}}{57.3} \right) \right]$$

The above three equations and those below require model states in the TIFS body axes systems:

$$\begin{aligned} p^* &= p \cos \theta_B + r \sin \theta_B = p_{MF} & V^* &= V \\ q^* &= q = q_{MF} & \beta^* &= \beta \\ r^* &= r \cos \theta_B - p \sin \theta_B = r_{MF} & \alpha^* &= \alpha - \theta_B \end{aligned}$$

The angular acceleration equations for \dot{p}^* , \dot{q}^* , \dot{r}^* are the same as the above with the dot variables substituted.

The following equations transform the model's V^* , α^* , β^* , \dot{V}^* , $\dot{\alpha}^*$, $\dot{\beta}^*$ at its CG to the values at the TIFS CG:

$$V_{MF} = \frac{1}{\cos \alpha_{MF} \cos \beta_{MF}} \left[V \cos \alpha^* \cos \beta + \frac{1}{57.3} (Z_{MTCG}^* q^* - Y_{MTCG}^* r^*) \right]$$

$$\sin \alpha_{MF} = \frac{1}{V_{MF} \cos \beta_{MF}} \left[V \cos \beta \sin \alpha^* + \frac{1}{57.3} (-X_{MTCG}^* q^* + Y_{MTCG}^* p^*) \right]$$

$$\alpha_{MF} = \arcsin [\sin \alpha_{MF}]$$

$$\sin \beta_{MF} = \frac{1}{V_{MF}} \left[V \sin \beta + \frac{1}{57.3} (X_{MTCG}^* r^* - Z_{MTCG}^* p^*) \right]$$

$$\beta_{MF} = \arcsin [\sin \beta_{MF}]$$

$$\begin{aligned} \dot{V}_{MF} &= \frac{1}{\cos \alpha_{MF} \cos \beta_{MF}} \left[\dot{V} \cos \alpha^* \cos \beta - V \cos \alpha^* \sin \beta \frac{\dot{\beta}}{57.3} + \sin \alpha^* \cos \beta \frac{\dot{\alpha}}{57.3} \right. \\ &\quad + V_{MF} \cos \alpha_{MF} \sin \beta_{MF} \frac{\dot{\beta}_{MF}}{57.3} + \sin \alpha_{MF} \cos \beta_{MF} \frac{\dot{\alpha}_{MF}}{57.3} \\ &\quad \left. + \frac{1}{57.3} (Z_{MTCG}^* \dot{q}^* - Y_{MTCG}^* \dot{r}^*) \right] \end{aligned}$$

$$\dot{\alpha}_{MF} = \frac{1}{V_{MF} \cos \alpha_{MF} \cos \beta_{MF}} [\dot{\alpha} V \cos \alpha^* \cos \beta + \sin \alpha^* (\dot{V}(57.3) \cos \beta - V \sin \beta \dot{\beta})$$

$$- \sin \alpha_{MF} (\dot{V}_{MF}(57.3) \cos \beta_{MF} - V_{MF} \sin \beta_{MF} \dot{\beta}_{MF})$$

$$+ \{X_{MTCG}^*(-\dot{q})^* + Y_{MTCG}^*(\dot{p})^*\}]$$

$$\dot{\beta}_{MF} = \frac{1}{V_{MF} \cos \beta_{MF}} [V \cos \beta \dot{\beta} + \dot{V}(57.3) \sin \beta - \dot{V}_{MF}(57.3) \sin \beta_{MF}$$

$$+ \{X_{MTCG}^*(\dot{r})^* + Z_{MTCG}^*(-\dot{p})^*\}]$$

These equations were not manipulated further to allow direct computation of "MF" quantities. Rather, since the computer cycle time was short (12.5ms), the above relationships were used with past values of the "MF" quantities appearing on the right hand side. This introduced an additional time delay, but since the time was short it was judged insignificant in its effect on the experiment.

The equation form for direct computation is included in Appendix A for future reference.

The model Euler angles and flight path angle were transformed with the following equations:

$$\sin \theta_{MF} = \sin \theta^* = \sin \theta \cos \phi \sin \epsilon_{\beta} - \cos \theta \cos \phi \sin \epsilon_{\beta}$$

$$\sin \phi_{MF} = \sin \phi^* = \frac{\sin \phi \cos \theta}{\cos \theta_{MF}}$$

$$\sin \gamma_{MF} = \cos \beta_{MF} (\cos \alpha_{MF} \sin \theta_{MF} - \sin \alpha_{MF} \cos \theta_{MF} \cos \phi_{MF})$$

$$- \sin \beta_{MF} \cos \theta_{MF} \sin \phi_{MF}$$

3.3 CROSSWIND SIMULATION

An artificial crosswind can be simulated in the TIFS by the deflection of its side force surfaces with a programmed mismatch in sideslip between the model and the TIFS. In this way, the TIFS sets up a wings level constant sideslip which the model aerodynamics and evaluation pilot do not see. To the pilot, it appears as if he were flying in a crosswind with his airplane having a lateral velocity component with respect to his heading. During these simulations, the existing crosswinds were augmented by an artificial component to bring the perceived crosswind up to 15 knots which is the maximum obtainable while allowing for additional side force surface deflection for model-following purposes.

3.4 DATA RECORDED

The pilot comments and ratings were considered the primary data of the investigation and were recorded on a voice tape. The summary of these comments are presented in Section 4. In addition to voice tapes a 58 channel digital recorder was used to record signals of interest. These included:

1. Pilot inputs
2. Control surface motions
3. Aircraft states (Model and TIFS)
4. Radar altitude
5. Sink rate

A specific list of recorded variables is presented in Table 7.

Table 7
DIGITAL RECORDING LIST

Note:

- 1) Subscript MTCG refers to a model parameter transferred to the TIFS CG
- 2) Subscript MP refers to a model parameter at the pilot station
- 3) Subscript T refers to a TIFS parameter at its CG
- 4) Subscript TP refers to a TIFS parameter at the pilot station
- 5) Subscript MF refers to a model parameter used for model following
- 6) A Δ is an incremental parameter from its engage value

<u>Channel No.</u>	<u>Variable</u>
1	$\Delta\theta_{MF}$
2	$\Delta\theta_T$
3	q_{MF}
4	q_T
5	$\Delta\alpha_{MF}$
6	$\Delta\alpha_T$
7	ΔP_E (differential pressure in TIFS elevator actuator)
8	ΔV_M
9	ΔV
10	\dot{V}_{MF}
11	\dot{V}_T
12	$\Delta N_{Z_{MP}}$
13	$\Delta N_{Z_{TP}}$
14	$\delta_{e_{ST}}$ (TIFS elevator actuator strut)
15	\dot{h}
16	e_M

Table 7
DIGITAL RECORDING LIST (Cont'd)

<u>Channel No.</u>	<u>Variable</u>
17	$\sin \gamma_{MF}$
18	$N_{y_{MF}}$
19	N_{y_T}
20	P_{MF}
21	P_T
22	ϕ_{MF}
23	ϕ_T
24	r_{MF}
25	r_T
26	δ_{e_c} (TIFS elevator command)
27	N_{z_T}
28	β_{MF}
29	β_T
30	α gust component
31	β gust component
32	$h_{press.}$
33	$h_{Gear-right}$
34	$h_{Gear-left}$
35	Loc. Deviation
36	G.S. Deviation
37	$N_{y_{MP}}$

Table 7
DIGITAL RECORDING LIST (Concl'd)

<u>Channel No.</u>	<u>Variable</u>
38	$N_{y_{TP}}$
39	Touchdown Pulse
40	ΔP_a (differential pressure in TIFS aileron actuator)
41	$N_{z_{MF}}$
42	δ_y (TIFS sideforce)
43	δ_a (TIFS aileron)
44	δ_z (TIFS direct left flap)
45	δ_r (TIFS rudder)
46	δ_a (TIFS aileron)
47	δ_e (TIFS elevator)
48	δ_x (TIFS throttle)
49	$\Delta \delta_{e_s}$ (Model pilot pitch input)
50	δ_{e_c} (Model elevator)
51	δ_{H_c} (Model horizontal tail)
52	δ_{a_s} (Model pilot roll input)
53	δ_{r_p} (Model pilot rudder pedal input)
54	δ_{RC} (Model rudder)
55	Model following test signal
56	PLA (Model power lever angle)
57	δ_{AC} (Model aileron)
58	α_{MF}

Section 4

RESULTS

4.1 INTRODUCTION

This section presents the results of the evaluation flights. Included is a chronology of the evaluations including the task variables and pilot ratings. The evaluations are also grouped by configuration and presented with pilot comment summaries. Plots of Pilot Rating versus configuration variables are given. A discussion of the results and a potential criteria dealing with lateral pilot offset position effects are presented. The fidelity of the model following and its effects are also given. Finally, conclusions are presented.

4.2 EVALUATION CHRONOLOGY

Three flights were flown on 21 October 1983 out of Niagara Falls Air Force Base. Pilot A was the evaluation pilot on the first and third flights, and Pilot B was the pilot on the second flight. There was no turbulence during the first flight, but there was light turbulence for the last two flights. The following table presents a listing of each approach including configuration variables, task variables, and pilot ratings. The SCAS number refers to the roll SCAS which yielded the various effective roll mode time constants:

<u>SCAS</u>	Effective τ_R
1	.6 sec
2	1.2 sec
3	2.3 sec

The y_p refers to distance that the pilot was offset to left of the centerline of the model aircraft: 0, 30 (actually 29.13), or 50 feet. The direction of the 200 ft runway offset indicates whether the pilot lined up to the left (L) or right (R) of the centerline during the outer approach. The direction of the 15 kt crosswind indicates if it came from the left (L) or right (R). Approach type refers to either a low approach or a simulated landing approximately five to ten feet off the ground (LA) or a complete approach to a real

touchdown on the TIFS' wheels (TD). Approaches made early in a flight could not be completed to a possible TIFS wheels touchdown due to weight limitations. Two pilot ratings are given. One is for the approach portion only and the other is an overall rating including the touchdown task. Only approaches that were completed to a real touchdown were given overall ratings, as ratings given for simulated touchdowns without having to place the wheels on the ground were not considered realistic.

TWIN-FUSELAGE EVALUATION CHRONOLOGY

Flight #750

Winds: 100° @ 6 kt

Runway: NIAG-28

Evaluation Pilot: A

Turbulence: None

App. #	SCAS	-yp	200 ft. RW Offset	15 kt X-Wind	App. Type	Pilot Rating	
						App	Overall
1	2	50	L	R	LA	3	-
2	2	50	R	R		4	-
3	2	50	L	L		5	-
4	2	50	R	L		Abort-Yaw osc. at de-crab	
5	2	50	R	L		5.5	-
6	1	30	L	L		4	-
7	1	30	L	R		7	-
8	1	50	L	R		7	-
9	1	50	R	L		Abort-No PR	
10	1	50	R	L		6	-
11	2	50	R	L	▼	4	-
12	2	0	None	None	TD	2	2
13	2	30	None	None		2	2
14	2	50	R	L		3	4
15	2	50	L	R		3	3
16	3	50	L	R		3	4
17	3	50	R	L		3	4
18	1	0	R	L		4	6
19	1	0	L	R		4	7
20	2	0	L	R		2	3
21	2	0	R	L		2	3
22	3	30	R	L	▼	3	5

TWIN-FUSELAGE EVALUATION CHRONOLOGY

Flight #751

Winds: 100⁰ @ 13 kt

Runway: NIAG-10

Evaluation Pilot: B

Turbulence: Light

App. #	SCAS	-yp	200 ft. RW Offset	15 kt X-Wind	App. Type	Pilot Rating	
						App	Overall
1	2	30	L	R	LA	3	-
2	2	30	R	L		3	-
3	1	30	R	L		6	-
4	1	30	L	R		Abort- feel system jitter	
5	1	30	L	R		5	-
6	1	50	L	R		7	-
7	1	50	R	L		6	-
8	2	50	R	L		4	-
9	2	50	L	R		Abort- system dump in turb.	
10	2	50	L	R		4	-
11	2	0	L	R		3	-
12	2	0	R	L		3	-
13	3	0	R	L	▼	3	-
14	3	30	R	L	TD	4	5
15	3	0	R	L		3	3
16	2	50	L	R		4	4
17	2	50	R	L		4	4
18	1	50	R	L	▼	3	5
19	1	50	L	R	LA*	5	-
20	1	50	L	R	TD	5	6
21	3	50	L	R	TD	3	5

* LA to 60 ft - aircraft on runway

TWIN-FUSELAGE EVALUATION CHRONOLOGY

Flight #752 Winds: 50° to 100° @ 12 to 17 kt Runway: NIAG-10
 Evaluation Pilot: A Turbulence: Light

App. #	SCAS	-yp	200 ft. RW Offset	15 kt X-Wind	App. Type	Pilot Rating	
						App	Overall
1	3	50	L	None	LA	4	-
2	1	50	R	L		3	-
3	2	50	R	L		3	-
4	2	50	R	L		3	
5	2	0	R	L		2	-
6	3	0	L	R		2.5	-
7	1	0	R	L	▼	4	-
8	1	30	R	L	TD	3	6
9	3	50	L	R		2	3
10	2	50	L	R		3	3
11	2	30	L	R		3	3
12	2	30	L	R		2	3
13	1	30	L	R		2	4
14	1	30	L	L		2	4
15	3	30	L	R		2	3
16	3	30	L	L	▼	2	4.5

4.3 PILOT RATING AND COMMENT SUMMARY

The pilot ratings and comment summary are presented in the following tables. They are grouped by configuration (SCAS and y_p). Within each configuration they are listed in chronological order by each pilot. Also presented after these summaries are plots of Pilot Rating versus the configuration variables of lateral pilot position (Figures 17, 18, and 19) and SCAS effective roll mode time constant (Figures 20, 21, and 22). Plots are shown separately for the approach and overall ratings as there was a definite trend to down grade each configuration as the touchdown had to be made with its accompanying higher pilot gain.

SCAS	$-y_p$	Pilot	Pilot Rating		Pilot Comments
			App. Only	Overall with TD	
1	0	A	4	6	Don't notice N_z with inputs during airwork. Roll/yaw oscillation during decrab and flare, PIOR = 4
			4	7	Roll oscillation during flare, PIOR=6, could not do tight task. Up and Away it is OK.
			4	-	Had a lateral oscillation, PIOR = 4
	30	A	4	-	Had an airspeed problem, motions not as noticeable (compared to $y_p = 50$) Can see difference between $y_p = 50$ and 30. 30ft is definitely improved. Less pitching and N_z motion. No problem in baseleg roll-out but could not land on spot. Can see vertical motion with roll inputs. Task benign until flare. Left offset and right x-wind hardest to do.
			7	-	
			3	6	Got into some oscillations in pitch and roll in flare, but easy to fly up and away with lower gain.
			2	4	Liked way airplane handled up and away, but down low it was too quick when I started getting into ailerons during X-wind correction. I also am getting into pitch axis due to my perceived motion relative to ground. Have to extract myself from the loop.
			2	4	Had a little bobble (oscillation) in the flare. Had to get out of the loop.
	8	B	6	-	In flare, strange feeling when I roll. I felt a heave-unnatural. Almost felt like I was losing control one time. May have maneuvered too aggressively. Don't feel the heave with roll inputs up and away.
5			-	Aborted last try due to feel system jitter with too aggressive control. This approach I had a slight PIO after I rolled out-roll/pitch combination. When I roll right I have to push and when I roll left I have to pull.	

SCAS	-yp	Pilot	Pilot Rating		Pilot Comments
			App. Only	Overall with TD	
1 TR=.6	50	A	7	-	When putting wing down in x-wind correction, I see pitch deviations and then I make pitch corrections which are not necessary.
			6	-	Would not be able to touchdown on a spot. Getting a solution on roll, pitch, throttle is problem.
			3	-	A lot of roll and heave activity on approach No problem with alignment, but in flare was concerned with cutting throttle so do not get into roll axis. Gave Airwork a PR=2. It was relatively crisp response for a large airplane. No perceptible N_z for gentle rolls. This had more precise and predictable bank control than previous (SCAS-3).
		B	7	-	Very noticeable heave with roll inputs. Roll PIO in offset correction, looks like unwanted roll inputs from control system when wings are level.
			6	-	Second approach, little better, tried making smaller inputs to reduce heave, but still got into roll oscillation down low, hard to make small roll corrections, response bigger than what I want.
			3	5	Trying to make gentler inputs at altitude to keep aircraft quiet. Notice thrust surges more with roll inputs. No problem with approach until flare. Also floated long in flare.
			5	-	Abort at 60 ft due to airplane on runway. Problems in approach when correcting for gusts.
			5	6	Gives impression of lunging and plunging in big turns. Got heave during roll correction in flare. Don't like altitude changes with roll corrections.

SCAS	-y _p	Pilot	Pilot Rating		Pilot Comments
			App. Only	Overall with TD	
2	0	A	2	2	No comments-just very good approach.
			2	3	Definitely better airplane than previous configuration (SCAS-1 with y _p = 0). Long landing due to power control problem.
			2	3	Only a little problem with yaw in flare.
			2	-	Crisp and predictable in roll. Alignment, decrab, and flare all worked well. I like it. Small pitch bobble near TD.
	B	3	-	No problem with x-wind correction.	
		3	-	Initial part of approach is pleasant. Airplane does what I want, when I want. Felt good, but have to have x-wind correction right the first time.	
	30	A	2	2	No apparent difference between 0 and 30 feet pilot offset with no alignment or x-wind correction made.
			3	3	Not much of a task without x-wind.
			2	3	had good solution all the way down, did not have to get into it laterally.
		B	3	-	Not a lot of workload on sidestep and x-wind maneuver. Don't notice that I'm offset 30 feet.
3	-		Nice flying airplane. Some problems in learning to use throttles properly, so landed long and slow.		

SCAS	-y _p	Pilot	Pilot Rating		Pilot Comments
			App. Only	Overall with TD	
2 τ _R = 1.2	50	A	3	-	For small inputs- no perceptable N _z . For big airplane type inputs - no distracting motions. Slight bump in the seat for rapid inputs, can perceive loss of altitude when I roll out left.
			4	-	Correcting from right side a little more difficult.
			5	-	Nose tends to wander a little during x-wind correction workload goes up near end of approach.
			5.5	-	Abort one approach due to yaw oscillation during decrab. This one had an altitude control problem. Could not tell if it was due to pilot position or pitch control system.
			4	-	Ballooned in flare.
			3	4	Did not feel I had to work that hard in getting it solved as some others.
			3	3	Was careful to stay out of roll axis after x-wind correction and made task easier.
			3	-	Airwork PR = 2, falls between other SCAS's (1 and 3 @ y _p = -50). On approach noticed sinking when rolling to align.
			3	-	Note sinking when aligning. Good until flare, then pilot gain (workload) goes up.
			3	3	No problem, middle of the road airplane.
		B	4	-	Don't notice any PIO tendency with this configuration.
			4	-	No trouble getting it to centerline, slight difficulty in flare.
			4	4	Pitch motions with roll inputs not that bad. Use low pilot gain. Have to concentrate on being gentle. Final line-up is hardest part.
			4	4	Same as previous approach. As long as I am aware I am in a big airplane and deliberately don't make big inputs, I don't get into trouble.

SCAS	-yp	Pilot	Pilot Rating		Pilot Comments	
			App. Only	Overall with TD		
3	0	A	2.5	-	Wanders a little in roll. Less predictable (than SCAS-2) in roll. Had a little lateral oscillation in roll in alignment.	
		B	3	-	Felt like a real airplane, best of the day. Did what I wanted it to do. Performance what I wanted.	
			3	3	Felt good, noticed that I was not offset from centerline of aircraft.	
	30	A		3	5	For small inputs up and away, motions are benign. Can definitely see altitude changes with roll inputs in flare and that changes the way I put pitch inputs in.
				2	3	Not as quick as others in roll.
				2	4.5	Did not notice any pilot up and down motion during corrections, but had some problems with ailerons on this approach.
		B	4	5	Down rated due to altitude change and slight thrust surge with roll inputs. Also requires a lot of rudder.	
	50	A		3	4	Lost a good solution due to roll input at end. Don't really notice N_z response though.
				3	4	Worked a little harder on this approach, but still had a little crab angle at TD. Have to stay off ailerons.
				4	-	Airwork PR=3. Laterally is loose. For small inputs requires more than I would like to get it rolling and then I have to counter it to stop. Poor predictability, did not know when roll would stop. Don't notice N_z at pilot station. In approach where I have to be in and out of the roll control more and have to be more precise than up and away, the looseness degrades PR to 4.
				2	3	Can feel cockpit come up when I roll out rapidly. But the more you have to correct for the x-wind the more trouble you get into on flare. If you have to use ailerons in the flare it affects how you fly.
		B	3	5	Feels fine on approach. Landing is a tough maneuver. Notice altitude changes with roll inputs.	

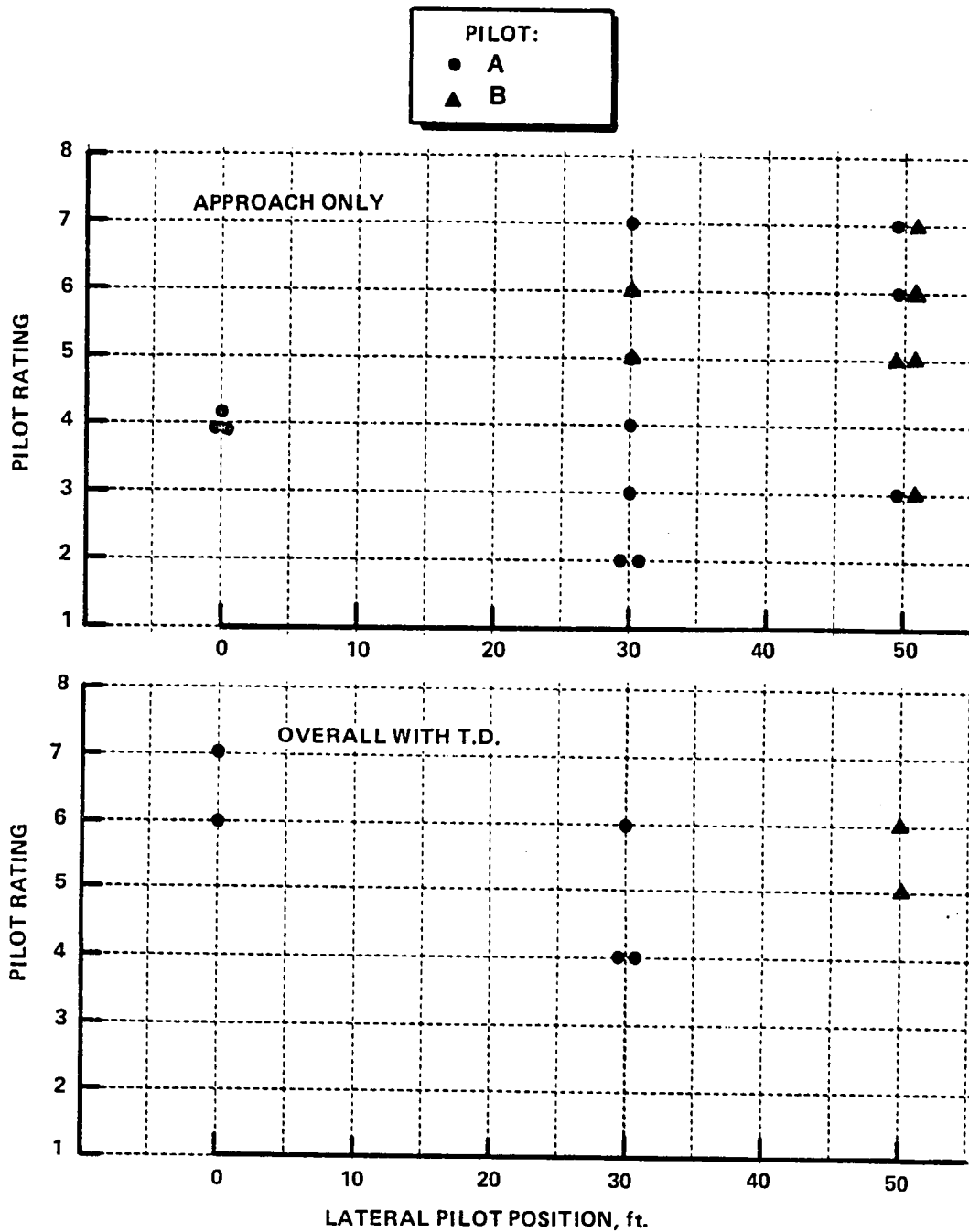


Figure 17 PILOT RATING VERSUS PILOT POSITION, ($\tau_R = 0.6$ sec)

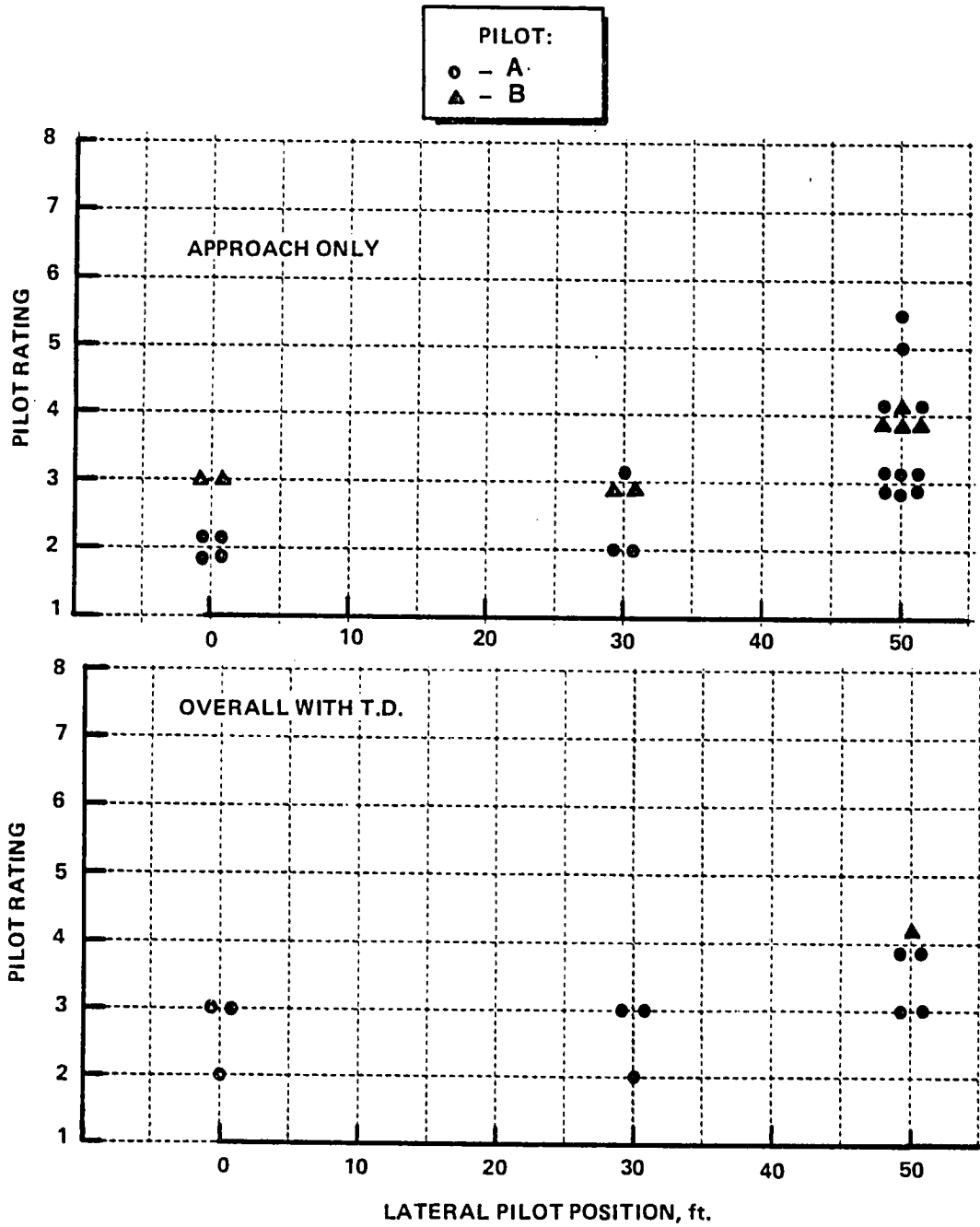


Figure 18 PILOT RATING VERSUS PILOT POSITION, ($\tau_R = 1.2$ sec)

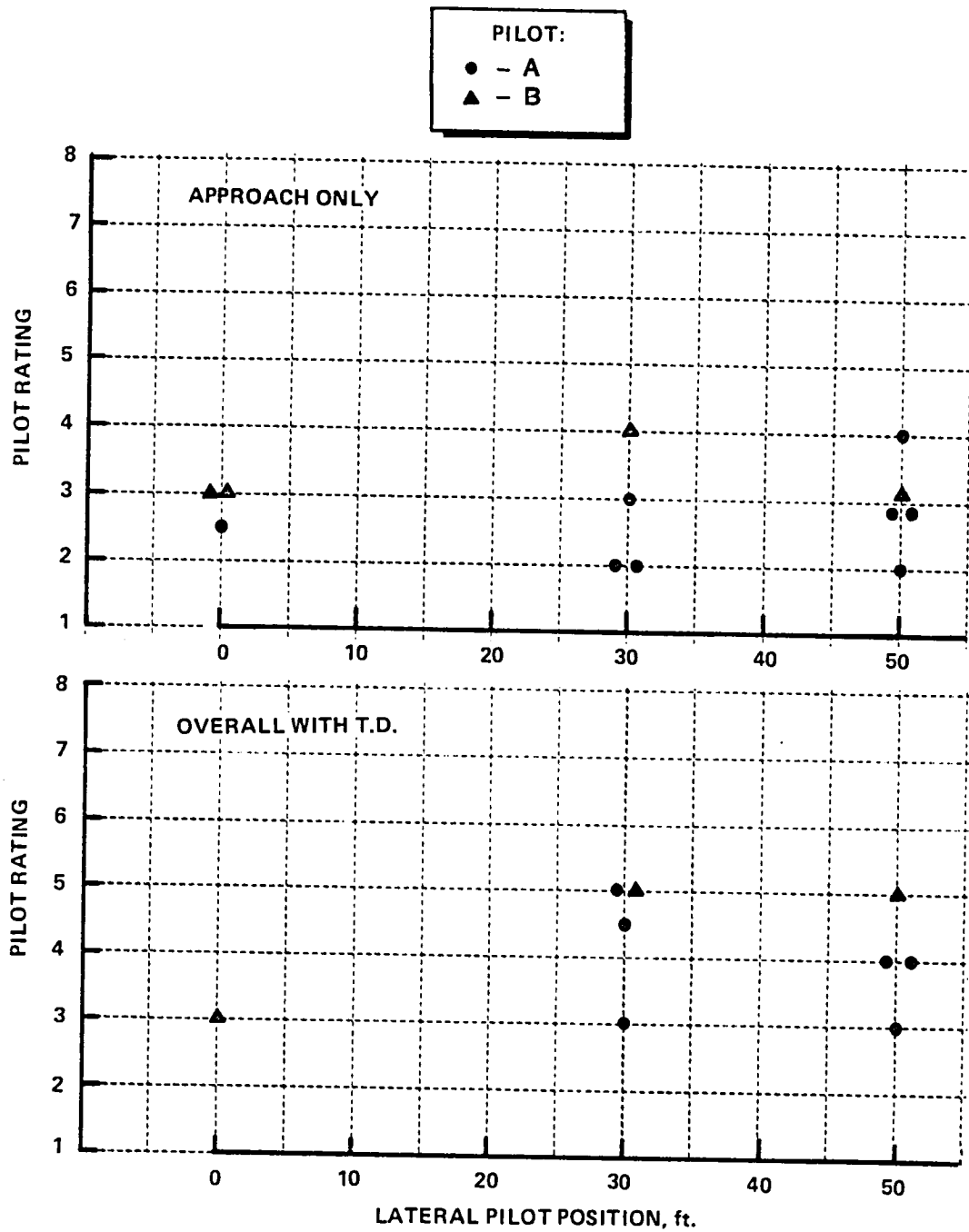


Figure 19 PILOT RATING VERSUS PILOT POSITION, ($\tau_R = 2.3$ sec)

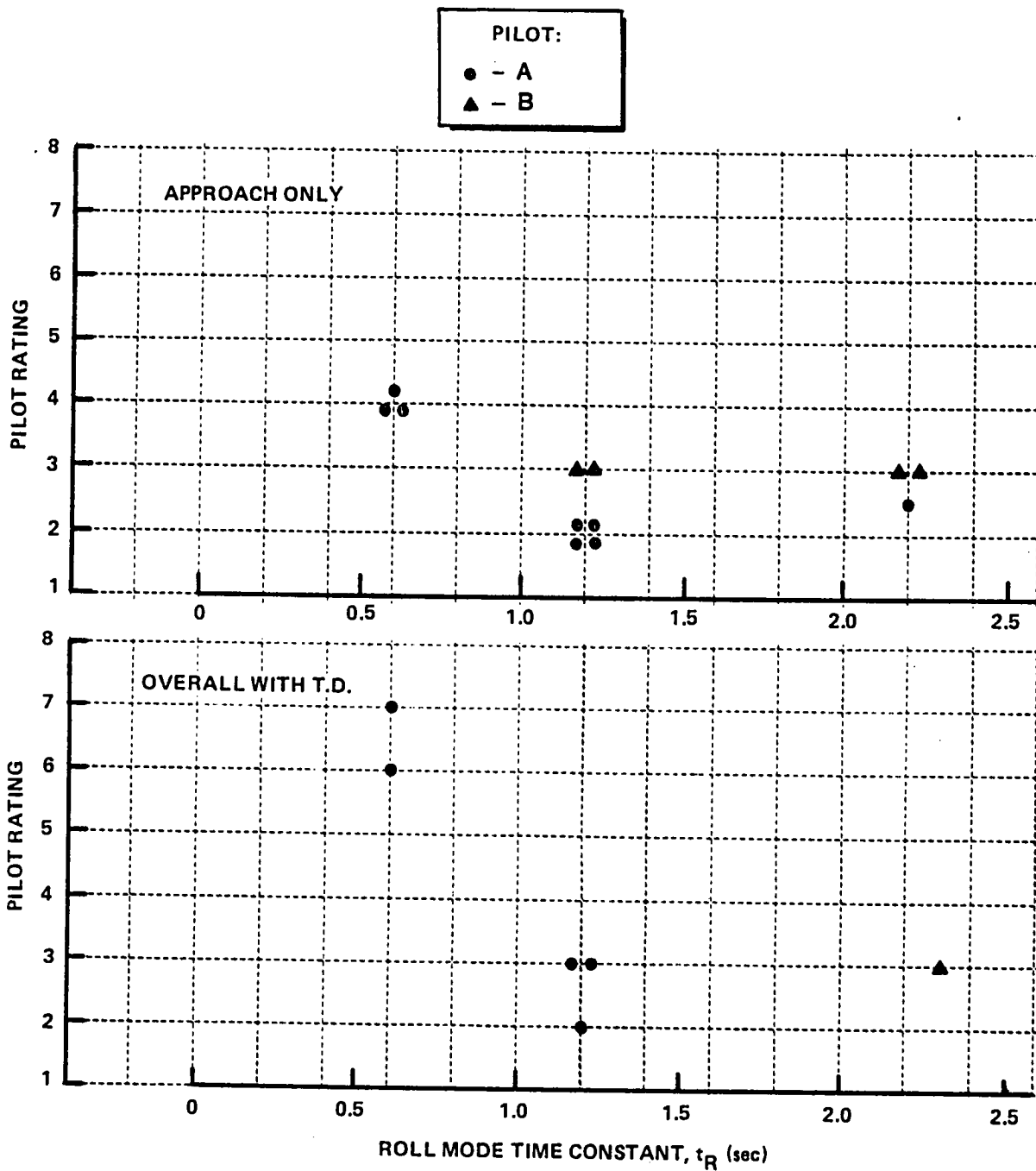


Figure 20 PILOT RATING VERSUS $\tilde{\zeta}_R$. ($Y_P = 0$. ft)

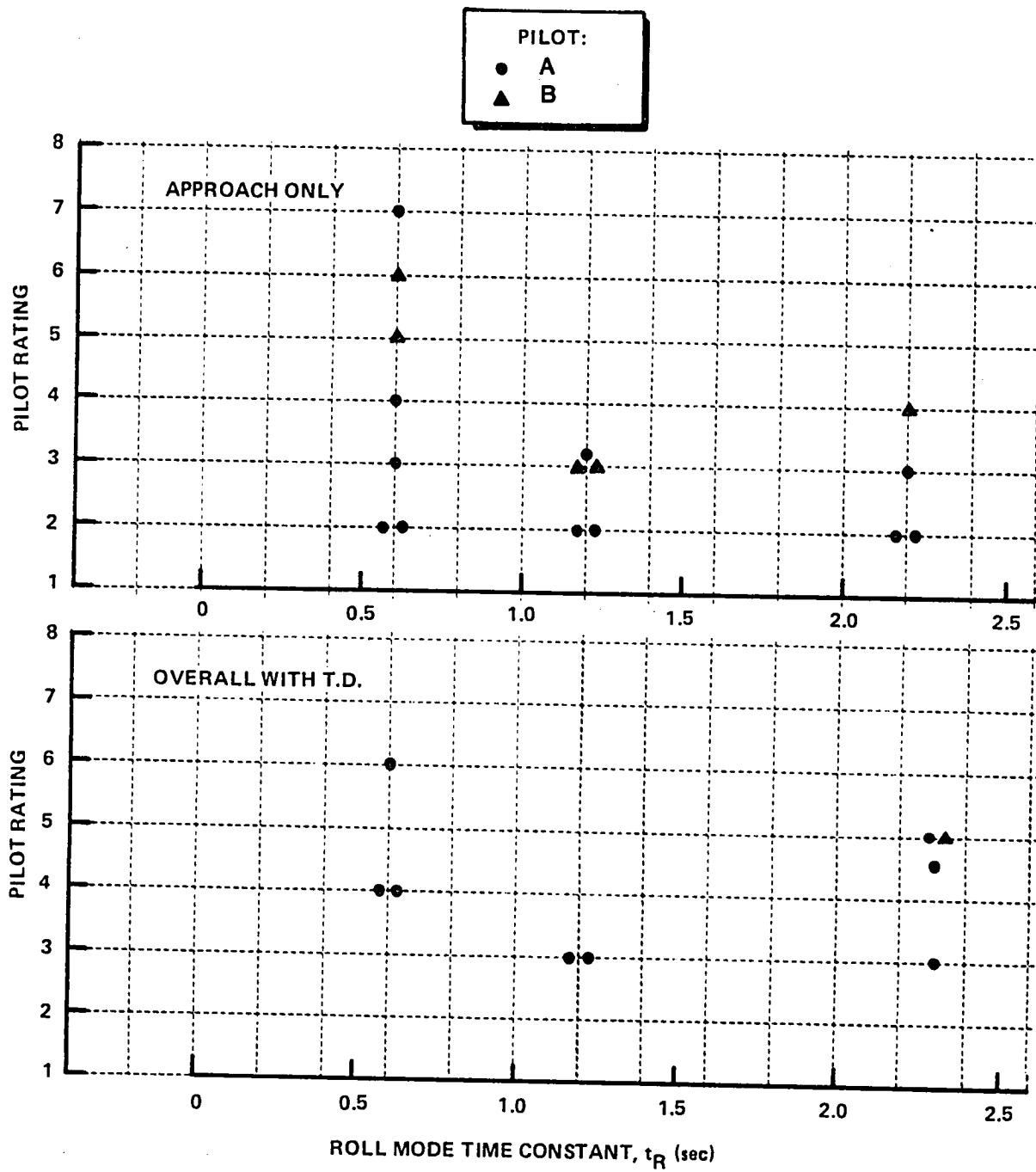


Figure 21 PILOT RATING VERSUS \tilde{z}_R ($Y_p = -30$ ft)

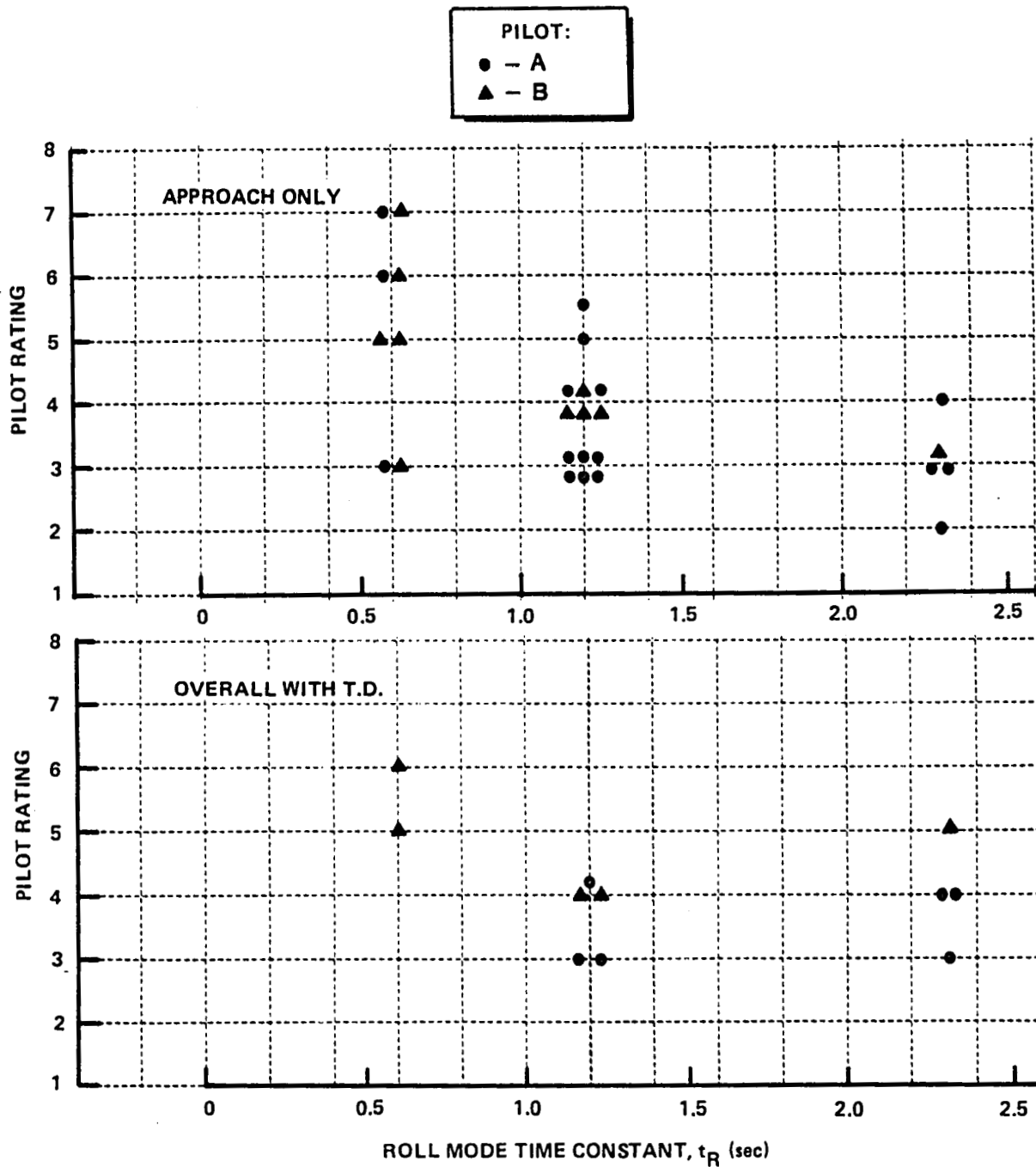


Figure 22 PILOT RATING VERSUS t_R , ($Y_p = -50$ ft)

4.4 POST - FLIGHT WRITTEN PILOT COMMENTS

The following are post-flight written pilot comments that covered the general impression of the evaluation pilots on the conduct and results of their flights.

Pilot A:

These notes reflect my observations noted during an airborne simulation of a twin-fuselage transport aircraft. Three flights, approximately 5-flight hours, were used to validate the system and fly the evaluations. The controlled variables, exclusive of flight control system design, included lateral pilot position from the center-of-gravity, crosswind velocity, and aircraft lateral displacement relative to the runway centerline as the aircraft approached decision height. Other important factors included the point at which the evaluation pilot began a sidestep maneuver to align the aircraft with the runway; the timing for auto-throttle disengagement; the crosswind landing technique used; and the gain used by the pilot during the task or subtask.

The evaluation pilot's task was to fly a rectangular pattern in visual meteorological conditions (VMC) and intercept either the ILS localizer and glideslope or visual final approach course and glideslope approximately 3 nautical miles from the runway threshold. Using visual references the pilot aligned the aircraft right or left of the final approach course and maintained this relative position until approximately 4-5000 feet from the beginning of the desired touchdown zone. At this point a sidestep maneuver was accomplished to align the aircraft with the runway centerline, and as the aircraft descended the flare was begun to decrease the rate of descent. Also for those test points involving crosswinds the lateral drift was zeroed by applying crosswind landing controls (rudder for runway centerline alignment and aileron into the wind). Dependent on fuel on board, some test points were flown to actual touchdown while others were flown to a simulated touchdown determined by the computed cockpit height at touchdown of the modeled aircraft. The task presented a satisfactory environment to evaluate cockpit motions in the simulated twin-fuselage configuration.

For all configurations flown, the handling qualities and cockpit motions of the simulated aircraft were satisfactory during transport type maneuvering in the approach phase prior to approaching decision height. The lateral displacement of the simulated pilot position from the center of gravity caused a variation in the cockpit motion as expected, but there was no significant increase in perceived normal acceleration for normal control inputs. Although small in magnitude the apparent vertical motion of the cockpit was much more obvious to the evaluation pilot, especially during the portion of the approach below decision height.

This was especially noticeable when making lateral control inputs as the aircraft was aligned with the runway just prior to touchdown. Because of the difficulty in precisely predicting aircraft directional response to rudder inputs, the pilot chose to use the "wing-low" crosswind landing technique. As the airspeed changed and the aircraft reactions to ground effect occurred, the amount of lateral control required for a stable solution changed. The evaluation pilot perceived a small vertical motion at the cockpit when these lateral control inputs were made. Coincident with these inputs, the flare for landing had begun, and this required elevator inputs which also caused some vertical motion at the pilot's station. The evaluation pilot had to distinguish between responses caused by the two control inputs.

During the flare maneuver used to land an aircraft, the pilot uses several feedback parameters to accomplish the task of landing the aircraft. His control inputs are conditioned responses to these parameters and their rate of change. So, if while flaring the aircraft and changing angle of bank the pilot perceives a change in the cockpit descent rate, he makes an elevator input to correct back to the desired rate. This may complicate the task, especially if the angle of bank change is stopped or reversed. It was difficult to land the aircraft in the desired touchdown zone when the test point included a crosswind.

Initially, there was no plan to include accurate touchdowns in the evaluation task. This was added when we realized that by including it, the gain of the evaluation pilot was increased as he attempted to meet the required touchdown parameters in the desired landing zone. As his gain

increased he was forced to make his control inputs in a somewhat reaction-type mode thus highlighting the results described above.

These results are not necessarily applicable to all high gain tasks. For example, if the task had been to track an ILS to touchdown using pitch and bank steering bars - a task that minimizes eye contact with the environment outside the cockpit - the comments would probably reflect a less degrading effect on pilot rating. Most of the pilot comments during this short evaluation appeared to indicate a definite difference between perceived up and away flying qualities and those in the later portion of an approach to touchdown where the primary sense used by the pilot is visual. Also the ratings seem to indicate the pilot's familiarity with the airplane was a factor.

To summarize, in up-and-away flight during normal passenger and transport aircraft type maneuvering, all configurations flown were satisfactory. During the flare for landing task, however, difficulties were encountered by the evaluation pilot in precisely controlling the rate of descent to touchdown in the desired landing zone.

Pilot B:

Comments are general - for specific comments, see tapes recorded during flight. The TIFS program was a quick look at a lot of cases where variables included pilot distance from centerline (30 or 50 ft), left or right approach misalignment, crosswinds, left and right, and values of SCAS. It was a lot of work to do in a short time. My preference for the evaluation would have been to do only 10 - 12 cases per flight. There was little time to consider the previous approach for grading before starting the next one, and there was little time to look at the airplane because the circuits were so short. Nevertheless, the grades probably show valid trends for the cases flown.

Concerning pilot offset - in general, thirty feet was not noticeably different from being on centerline. Fifty feet was noticeable in some cases out not all.

One of the most significant aspects of the simulation was the cyclic engine surging and related vertical accelerations from the direct lift flap

system (DLF). This was particularly true in natural turbulence, the condition which prevailed during the bulk of my rating cases. The cyclic engine sound and vertical accelerations invited a pilot participation which, at times, became a PIO situation. There were a few times when the engine surge sounds almost acted like a metronome indicating to the pilot when to push and when to pull. I am not convinced that this simulation facet did not influence behavior of the aircraft and therefore ratings.

The basic control system, rate command attitude hold was excellent. Minimal pilot in the loop was required for desired results. No task was encountered which could not be handled, however, a conscious effort had to be made to make deliberate calculated inputs. Rapid control inputs based on hasty decisions were never acceptable and could not be used.

No combination of variables proved too difficult to fly the airplane around the pattern on to final (offset) and even recover from the offset and align the airplane centerline with the runway centerline. From that point on, troubles began depending on the variables, turbulence, engine surge/airplane heave problem. The transition to flare and landing was the most taxing facet of the task (especially if the touchdown was to be made at a specific point on the runway). I am not sure when this was a real problem; was it a function of the simulated airplane, or the simulation trying to be the airplane? Individual comments for each run may reveal which, when compared to the status of the variables. At any rate, I think that training and practice could overcome many of the problems I had with some of the worst cases. (Improve the worst ratings.)

Ride qualities did not appear to be a problem with me, but other crewmembers had comments regarding the effects of various combinations of variables on ride qualities. Perhaps that is more of a factor than the pilot's ability to fly the task.

Based on my meager experience in this program, I would suggest that with an adequate control system properly tuned, the piloting task is no worse flying from a 30-foot offset pilot position than flying from a centerline position. (If and when such an aircraft appears on the scene my guess is that

it will be an all electric machine with Cooper-Harper ratings of 1 for all tasks.) I'm not sure about the 50-foot offset. That one may be a little troublesome. However, I suspect that the real problems with a real airplane will be physical limitations due to geometry, size, weight, etc. or ride quality considerations. They will manifest themselves before the piloting problems show up.

4.5 DISCUSSION OF RESULTS

A quick review of the pilot rating data and plots shows much scatter. However, there are some significant results which are apparent when a thorough examination of the ratings and comments are made.

• Baseline Configuration

First of all the configuration which can be considered as a baseline conventional airplane, SCAS-2 ($\tau_R = 1.2$ sec) with $y_D = 0$ ft, was solidly rated a level 1 airplane. Pilot ratings of 2's and 3's were given during six separate evaluation approaches, three of which went to actual touchdowns. This indicated that the configuration was a good one about which the experimental variations of pilot position and roll mode time constant could be made. Any characteristics or problems that were brought out by the evaluation pilots should be due to the experiment variables and not some underlying problem in the baseline configuration. The only mildly unpleasant features dealt with learning how and when to use the throttle in controlling airspeed and learning how to use the rudders to decrab the aircraft for landing in a crosswind.

• Roll Mode Time Constant Effect

There is a definite trend in pilot ratings versus roll mode time constant. From the overall ratings shown in Figures 20, 21, and 22 it can be seen that the mid-value τ_R of 1.2 sec for SCAS-2 consistently received the best ratings, no matter what the pilot position was. The fast τ_R of .6 sec for SCAS-1 received significantly poorer ratings while the rating for the slow τ_R of 2.3 sec for SCAS-3 were only slightly worse than those for $\tau_R = 1.2$ sec. when the pilot was on the centerline of the aircraft with $\tau_R = .6$ the pilot gave ratings of 6 and 7 for the two touchdown approaches. Comments indicated

that severe roll/yaw oscillation ($PIOR = 4$ and 6) occurred when ever the pilot tried to do a high gain task such as a flare and spot landing. Up and away the aircraft was fine.

As the pilot position was moved off the centerline with the fast τ_R of .6 sec, the normal accelerations that went along with roll inputs compounded the roll control problem. Though this is not apparent in the pilot ratings for touchdown, there is much scatter in the approach only ratings with the pilot at 30 or 50 feet (see Figure 17). Ratings from 2 to 7 were given. This wide range of pilot ratings indicates that the configuration is very highly task dependent. If the pilot can use low gain and make gentle maneuvers the configuration will be rated highly. However, as the workload goes up and quick maneuvers must be made, the ratings deteriorate rapidly. There were many comments dealing with the necessity of staying out of the roll loop to avoid PIO 's. The pilots mentioned the disturbing vertical motions associated with the pilot position as being "unnatural" and yielding a "plunging and lunging" impression with large inputs. These comments indicated that the vertical motions were much worse at 50 feet than at 30 feet. At times the pitch and vertical cues observed by the pilot during roll corrections prompted him to make unnecessary pitch inputs. With the pitch rate command/attitude hold control system these unnecessary pitch inputs could easily disturb an approach that had been set up properly. The outcome could be a ballooning flare and a long float or a hard landing.

Both the τ_R 's of .6 sec and 1.2 sec are Level 1 (see Figure 11 page 2-24 for definition of Levels) according to the Military Flying Qualities Specification, MIL-F-8785C, which states that Level 1 τ_R 's must be less than 1.4 sec while Level 2 τ_R 's lie between 1.4 and 3.0 sec. However, the above results indicate that .6 seconds may be near the lower limit of satisfactory roll mode time constants for large airplanes. The problems seen with the fast roll mode in this experiment are similar to those seen in the in-flight investigation of fighter configurations done in Reference 4. The results of that study showed that roll ratcheting and PIO 's could occur in high gain tasks when τ_R was reduced to less than .25 sec due to abrupt roll response. A similar phenomenon may be happening with the present large airplane configurations, though not deteriorating to a ratcheting problem.

The slow roll mode time constant configuration, SCAS-3, $\tau_R = 2.3$ sec yielded generally borderline Level 1-2 pilot ratings (see Figure 19). This would be expected as the MIL-F-8785C level 2 region for τ_R is between 1.4 and 3.0 seconds. Pilot comments indicated a "looseness" in roll control and that it was less predictable than the other configurations. The most interesting feature of these slower roll mode configurations is that the pilot ratings do not get worse as the pilot position is shifted off of the airplane centerline. The pilot ratings remain in the 3 to 5 region for all pilot ratings and the comments are similar. The pilots did notice altitude changes with roll inputs but did not feel they were significant enough to degrade their ratings. It appears that it is the normal acceleration rather than just vertical displacement during rolling maneuvers which cause problems. The actual altitude change at a specific pilot position is the same for each SCAS for a given roll attitude change. However, the normal acceleration is proportional to the inverse of the roll mode time constant, as the \dot{p} and therefore, $n_{z_p} = (\dot{p}) \cdot (y_p)$ increase with decreasing values of roll mode time constant. With slow τ_R , the normal accelerations are low enough that they do not affect the ratings even with the pilot offset 50 feet (see Figure 19). With the mid-value τ_R the pilot ratings begin to degrade at the 50 foot position (see Figure 18). With the fast roll mode constants the ratings degrade at the 30 foot position for the approach ratings and are poor in the touchdown even at the centerline pilot location (see Figure 17).

o Pilot Position Effect

Most of the results presented here were really discussed in the previous section on the effects of roll mode time constant. The effects of the pilot position and roll mode are highly inter-related. For all of the SCAS configurations the pilot comments indicate that the pilots noticed the effect of being 30 or 50 feet off the centerline with larger effects being noted at 50 feet. The effects were manifested through perceived altitude changes with roll inputs for all SCAS configurations. These effects were more apparent near the ground than up and away. With the slow τ_R of 2.3 sec, though the pilot noted the offset, it did not affect his ratings or comments (see Figure 22). However, as the τ_R was decreased to 1.2 sec and then .6 sec the pilot

offset position had significant effects on pilot ratings and comments. As was mentioned previously, it appears as if normal acceleration during rolling maneuvers rather than just vertical displacement is the driver of poor flying qualities. The pilot has to be 50 feet offset from the centerline with $\tau_R = 1.2$ sec before pilot ratings degrade into the Level 2 region. With $\tau_R = .6$, the pilot ratings of near Level 3 were received at all pilot positions for high gain pilot tasks.

- Learning Effect

The chronological table of ratings in Section 4.3 shows significant improvement in rating with time in Pilot A's ratings of SCAS 1 at 30 feet and at 50 feet. The rest of the data show essentially no change with repeat runs. Since both pilots commented on the large number of configurations seen in a short time and the feeling that they were able to perform better as they had more experience, there was probably some learning present. However, the ratings do not reflect this, in general.

4.6 POTENTIAL CRITERIA FOR LATERAL PILOT OFFSET POSITION EFFECTS

It has been postulated that the normal acceleration experienced by the pilot during rolling maneuvers is the characteristic that causes problems when the pilot is laterally offset from the airplane centerline. A parameter which may give a measure of this effect is the ratio between the maximum incremental normal acceleration experienced at the pilot station and the steady state roll rate for a step roll input: $\Delta n_{z_p}/p_{SS}$. This is similar to the lateral acceleration parameter: $\Delta n_{y_p}/p$ which was developed during an in-flight simulation experiment dealing with very long supersonic cruise aircraft configurations (Reference 1). The pilot position was far forward and above the aircraft's center of rotation for rolling maneuvers and experienced large lateral accelerations which degraded the flying qualities.

The values of $\Delta n_{z_p}/p_{SS}$ were calculated for each of the configurations flown from the step response time histories shown in Section 2. The results are shown in Table 8 along with the range of pilot ratings given for each configuration.

Table 8
NORMAL ACCELERATION PER ROLL RATE PARAMETER

SCAS	τ_R (sec)	$-y_p$ (ft)	$\Delta n_{z_p}/p_{ss}$ (g/deg/sec)	Pilot Ratings	
				Overall with TD	Approach Only
1	.6	0	0	6-7	4
1	.6	30	.019	4-6	2-7
1	.6	50	.033	5-6	3-7
2	1.2	0	0	2-3	2-3
2	1.2	30	.011	2-3	2-3
2	1.2	50	.020	3-4	3-5.5
3	2.3	0	0	3	2.5-3
3	2.3	30	.006	3-5	2-4
3	2.3	50	.011	3-5	2-4

There is only a loose correlation between $\Delta n_{z_p}/p_{ss}$ and Pilot Rating due to the scatter of data. However, when neglecting the $y_p = 0$ configuration it may be postulated that values of $\Delta n_{z_p}/p_{ss}$ above .02 g/deg/sec will yield unsatisfactory ratings while values below .01 g/deg/sec will yield satisfactory ratings. It is interesting to note that the maximum values of the lateral acceleration parameter from the Reference 1 study for Level 1 was .012 g/deg/sec and for Level 2 was .035 g/deg/sec. Therefore, both of these sets of data indicate that maximum magnitude of linear acceleration that a pilot will tolerate during rolling maneuvers before it starts to deteriorate his ratings is in the neighborhood of .01 to .02 g/deg/sec.

4.7 MODEL FOLLOWING FIDELITY EFFECTS

The fidelity of the model following during this program was generally good. Some examples of typical runs where large roll maneuvers were made are shown in Figures 23, 24, and 25.

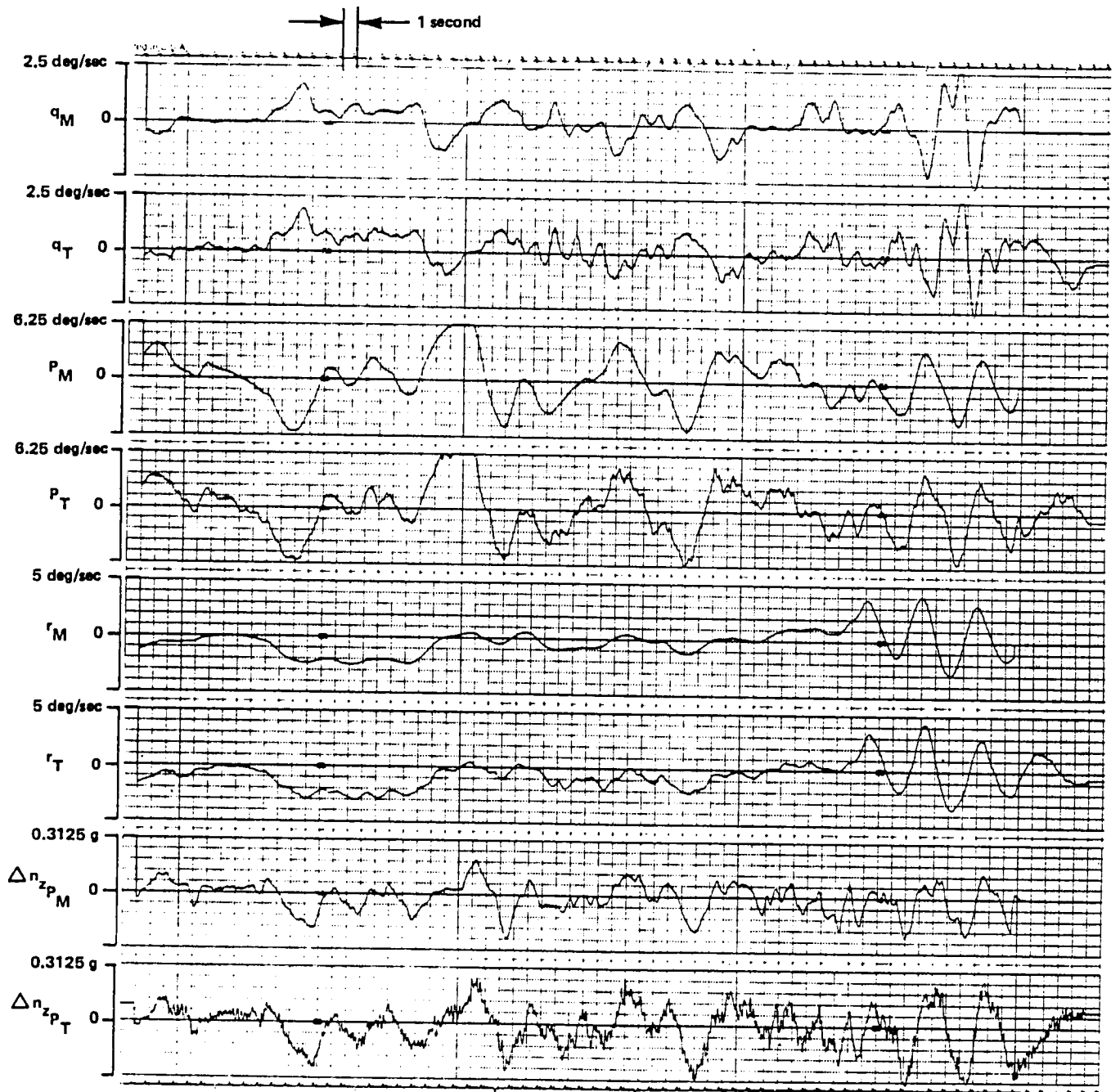


Figure 23 MODEL FOLLOWING, FLT 750, APPROACH 4, SCAS - 2, $Y_p = -50$ FT

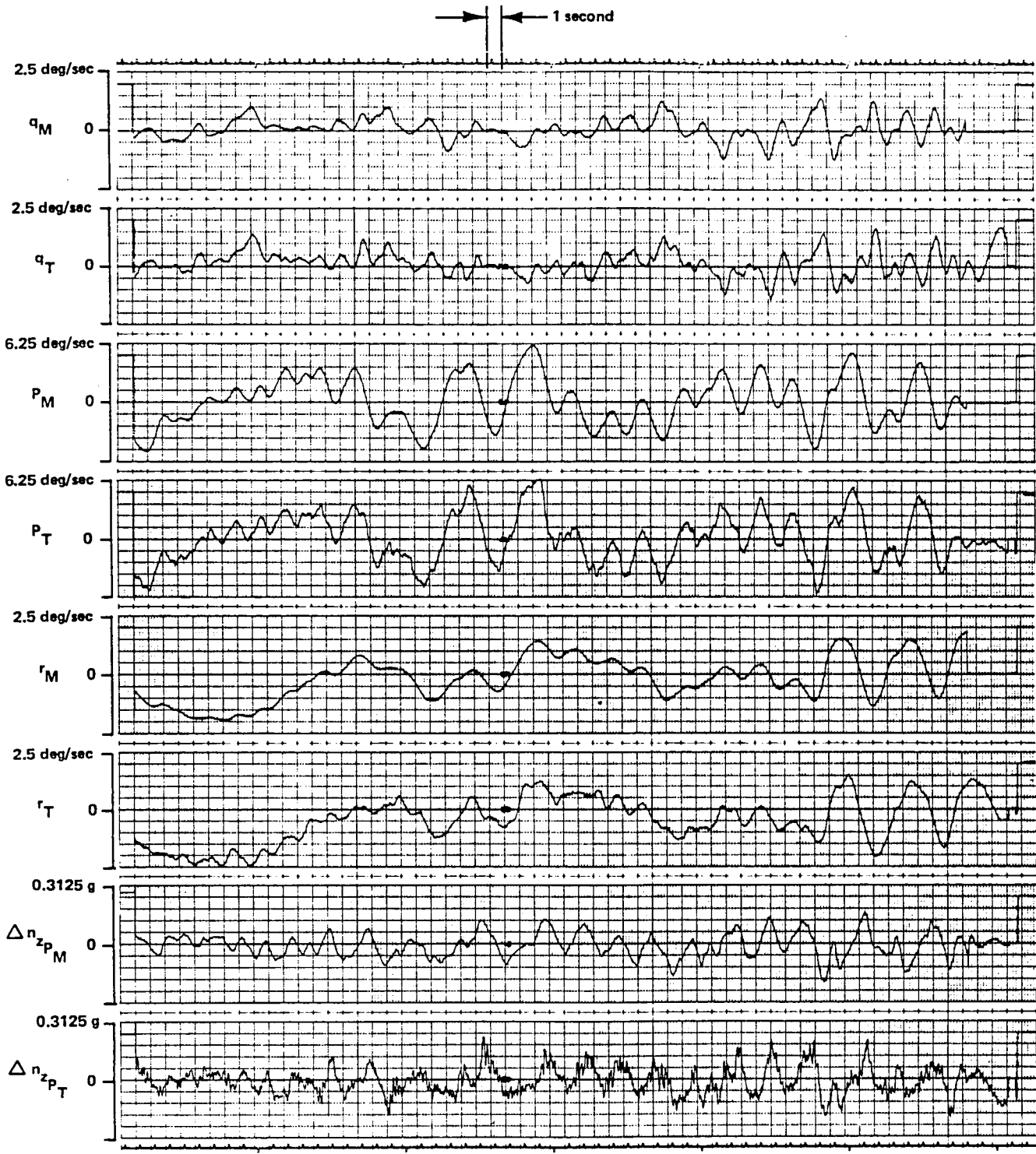


Figure 24 MODEL FOLLOWING, FLT 750, APPROACH 7, SCAS - 1, $Y_p = -30$ FT

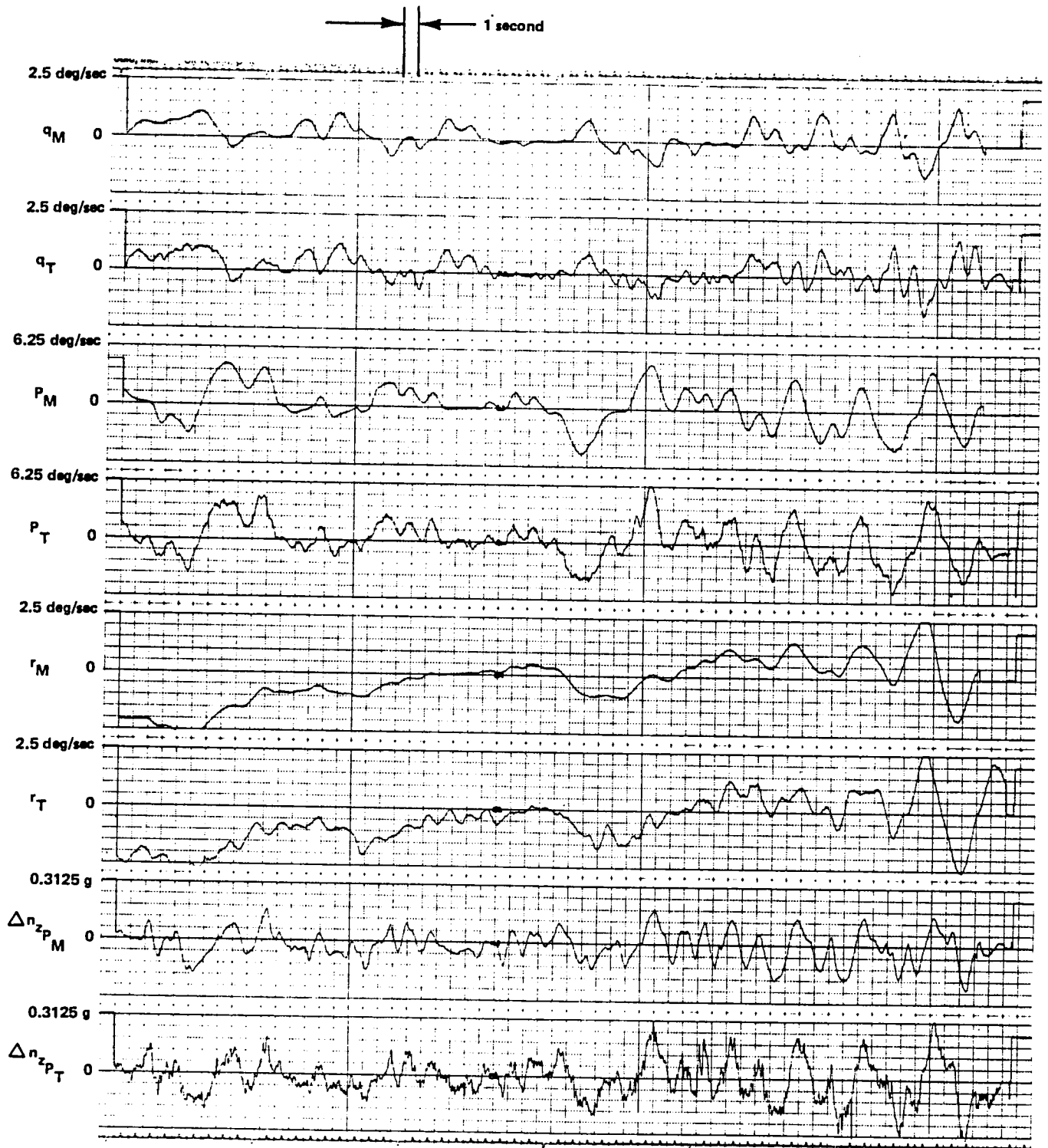


Figure 25 MODEL FOLLOWING, FLT 750, APPROACH 9, SCAS - 1, $Y_p = -50$ FT

There was one characteristic of the model following that did affect pilot comments. This dealt with the coupling in of the TIFS' throttle when roll inputs were made. As a roll input was made with the pilot offset from the model's centerline, a normal acceleration and altitude rate was generated in the model. This forced the direct lift flaps to move to match the vertical response. An unwanted by-product of the flap deflections was a drag change which produced velocity and longitudinal acceleration errors with respect to the model. These errors were fed back to the TIFS' throttles. Since the TIFS' throttles are of relatively low bandwidth the TIFS was not able to eliminate the V and V errors quickly. Sometimes a TIFS' throttle surge and oscillation occurred. This also happened occasionally in turbulence which produced velocity errors. The pilots noted this characteristic in their comments and it sometimes disturbed their control of velocity of the model. However, the matching of the pitch, roll, yaw, vertical, and lateral axes' responses was good so the evaluations of the flying qualities of the aircraft in these axes can be considered as proper.

An example of the throttle surging and oscillation with roll inputs can be seen in Figure 26. The large rolling maneuvers caused large normal acceleration excursions which were matched by the TIFS. These excursions are in phase with the V_{TIFS} oscillations due to the drag caused by the direct lift flaps. The V error then caused the TIFS' throttles to surge and oscillate as shown on the bottom track of the figure.

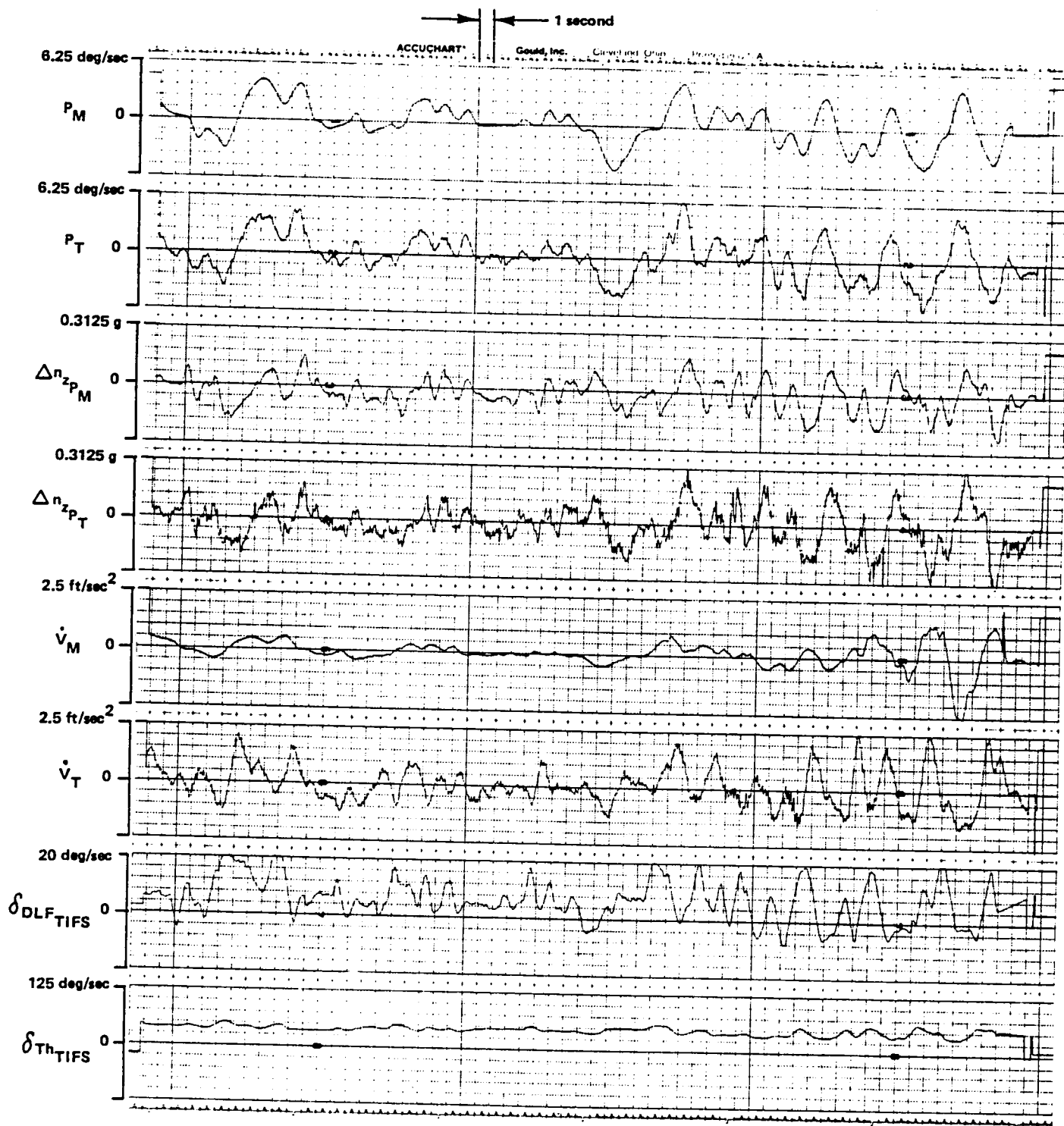


Figure 26 MODEL FOLLOWING WITH \dot{V} ERROR AND THROTTLE SURGING, FLT 750,
 APPROACH 9, SCAS - 1, $Y_p = 50$ FT

4.8 CONCLUSIONS AND RECOMMENDATIONS

- Lateral pilot position has a significant effect on pilot ratings and comments during landing approach and touchdown.
- Factors affecting these ratings are the actual distance that the pilot is offset from the centerline of the aircraft, roll mode time constant, and degree of difficulty of the landing task (crosswinds, turbulence, spot landing).
- For the baseline aircraft configuration and type of control system flown in this experiment a lateral pilot offset of 30 feet generally had little effect on pilot ratings while at 50 feet the ratings deteriorated.
- Roll mode time constant had a significant effect on pilot ratings and comments as the pilot moved further off the centerline. With $\tau_R = .6$ sec pilot comments indicated problems at an offset of 30 feet, while with $\tau_R = 2.3$ sec, there was no deterioration of pilot ratings or opinions even at 50 feet off the centerline.
- Problems that the pilots had with the large pilot offsets and fast roll mode time constants showed up as coupled roll and pitch oscillations. Pilots made unnecessary pitch inputs due to normal accelerations and vertical displacements observed at the offset pilot position during rolling maneuvers.
- A potential criteria for lateral pilot offset position effects deals with the ratio of the incremental normal acceleration at the pilot station to the steady state roll rate for a step input: $\Delta n_{z_p} / p_{SS}$. When the value of this parameter reaches .01 to .02 g/deg/sec a deterioration of pilot ratings and flying qualities can be expected.

- Both pilots commented on the large number of configurations seen in a short time and the presence of a learning curve. Although the pilot performance may have been influenced by learning, the trend is not reflected in the ratings, in general.
- At the time of these evaluations, the TIFS throttle controls occasionally produced undesired inputs in response to rapid drag changes in the model and in the TIFS itself. Evaluation pilot commentary indicates that there was a tendency to chase these inputs and produce PIO's, particularly in rough air. This anomaly was not a major factor in the experiment since the poor configurations were poor without throttle surging present and PIO tendencies were found that did not involve surging.
- Further research should be done to study various solutions to the problem of Δn_{z_p} when rolling such as offset roll axis and wings-level sidestep maneuvers using side force. The runway width requirement for aircraft of this type should also be defined.



Section 5
REFERENCES

1. Weingarten, N. C.: "An Investigation of Low Speed Lateral Acceleration Characteristics of Supersonic Cruise Transports Utilizing the Total In-Flight Simulator (TIFS)", NASA CR-159059 and Calspan Report No. 6241-F-2, July 1979
2. Weingarten, N. C. and Chalk, C. R.: "In-Flight Investigation of the Effects of Pilot Location and Control System Design on Airplane Flying Qualities for Approach and Landing", NASA-CR-163115 and Calspan Report No. 6645-F-7, December 1981
3. Reynolds, P. A.: "Capabilities of the Total In-Flight Simulator", AFFDL-TR-72-39, July 1972
4. Monagan, S. J., Smith, R. E., and Bailey, R. E.: "Lateral Flying Qualities of Highly Augmented Fighter Aircraft", AFWAL-TR-81-3171, March 1982



Appendix A
MODEL FOLLOWING CONTROL ALGORITHMS

The control algorithms in use for the twin-fuselage investigation are specified below in terms of linear gains. Some of these gains were fixed, some varied inversely with model indicated airspeed, V_{i_m} (kts), some varied inversely with model true airspeed, V_{T_m} (fps), and some varied inversely with model dynamic pressure, \bar{q}_m (psf).

The error gains multiply the difference between model motions at the TIFS center of gravity and TIFS motions - for example $\epsilon_\beta = \beta_{MF} - \beta$.

These gains were as follows:

$$\frac{\delta_e}{\epsilon_q} = -2.18 \frac{132^2}{V_{i_m}^2}, \text{ sec}$$

$$\frac{\delta_r}{\epsilon_\beta} = 3.03 \left(\frac{132}{V_{i_m}} \right), \text{ sec}$$

$$\frac{\delta_e}{\epsilon_\theta} = -5.45 \frac{132^2}{V_{i_m}^2}, \text{ ---}$$

$$\frac{\delta_z}{\epsilon_\alpha} = -1.20 \left(\frac{132}{V_{i_m}} \right), \text{ sec}$$

$$\frac{\delta_e}{J\epsilon_\theta} = -2.73 \frac{132^2}{V_{i_m}^2}, \text{ sec}^{-1}$$

$$\frac{\delta_z}{\epsilon_\alpha} = -8.06 \left(\frac{132}{V_{i_m}} \right), \text{ ---}$$

$$\frac{\delta_a}{\epsilon_p} = -2.80 \left(\frac{132}{V_{i_m}} \right), \text{ sec}$$

$$\frac{\delta_x}{\epsilon_v} = 4.13 \frac{132^2}{V_{i_m}^2}, \text{ \%/fps}^2$$

$$\frac{\delta_a}{\epsilon_\phi} = -3.94 \left(\frac{132}{V_{i_m}} \right), \text{ ---}$$

$$\frac{\delta_x}{\epsilon_v} = 9.07 \frac{132^2}{V_{i_m}^2}, \text{ \%/fps}$$

$$\frac{\delta_r}{\epsilon_r} = 0$$

$$V_{i_m} = 132 \text{ kts at trim}$$

$$\frac{\delta_r}{\epsilon_\beta} = 15.14 \left(\frac{132}{V_{i_m}} \right), \text{ ---}$$

The feedforward gains were as follows:

$$\frac{\delta_e}{\dot{q}_{MF}} = -.43 \frac{59.4}{\bar{q}_m}, \text{ sec}^2$$

$$\frac{\delta_r}{p_{MF}} = -1.03 \frac{b}{2V_{T_m}}, \text{ sec}$$

$$\frac{\delta_e}{\alpha_{MF}} = -.23, \text{ ---}$$

$$\frac{\delta_z}{n_{z_{MF}}} = -67.7 \frac{59.4}{\bar{q}}, \text{ deg/g}$$

$$\frac{\delta_e}{\delta_{z_{CFF}}} = -.08, \text{ ---}$$

$$\frac{\delta_z}{\alpha_{MF}} = -7.16, \text{ ---}$$

$$\frac{\delta_e}{\dot{q}_{MF}} = -16.5 \frac{c}{2V_{T_m}}, \text{ sec}$$

$$\frac{\delta_z}{\delta_{e_{CFF}}} = -.84, \text{ ---}$$

$$\frac{\delta_e}{\dot{\alpha}_{MF}} = -6.21 \frac{c}{2V_{T_m}}, \text{ sec}$$

$$\frac{\delta_x}{\dot{V}_{MF}} = 8.2, \text{ \%/fps}^2$$

$$\frac{\delta_a}{\dot{p}_{MF}} = -.99 \frac{59.4}{\bar{q}_m}, \text{ sec}^2$$

$$\frac{\delta_x}{\sin \gamma_{MF}} = 263, \text{ \%/---}$$

$$\frac{\delta_a}{\beta_{MF}} = -1.70, \text{ ---}$$

$$\frac{\delta_x}{\bar{q}_m} = .137, \text{ \%/psf}$$

$$\frac{\delta_a}{r_{MF}} = -3.13 \frac{b}{2V_{T_m}}, \text{ sec}$$

$$\frac{\delta_x}{\alpha_{MF}} = 1.97 \frac{\bar{q}}{59.4}, \text{ \%/deg}$$

$$\frac{\delta_a}{p_{MF}} = -8.80 \frac{b}{2V_{T_m}}, \text{ sec}$$

$$\frac{\delta_y}{n_{y_{MF}}} = 142.1 \frac{59.4}{\bar{q}}, \text{ deg/g}$$

$$\frac{\delta_a}{\delta_{r_{CFF}}} = -.19, \text{ ---}$$

$$\frac{\delta_y}{\beta_{MF}} = 3.04, \text{ ---}$$

$$\frac{\delta_r}{\dot{r}_{MF}} = -.71 \frac{59.4}{\bar{q}_m}, \text{ sec}$$

$$\frac{\delta_y}{r_{MT}} = -.38 \frac{b}{2V_{T_m}}, \text{ sec}$$

$$\frac{\delta_r}{\beta_{MF}} = .89 \quad , \text{ ---} \quad \frac{\delta_y}{\delta_{rCFF}} = -.63 \quad , \text{ ---}$$

$$\frac{\delta_r}{r_{MF}} = -1.26 \frac{b}{2V_{T_m}} \quad , \text{ sec} \quad \frac{\delta_y}{\delta_{aCFF}} = .03 \quad , \text{ ---}$$

$$\bar{q}_m = 59.4 \text{ psf at trim}$$

$$V_{T_m} = 223 \text{ fps at trim}$$

$$c = 9.52 \text{ ft}$$

$$b = 105.3 \text{ ft}$$

CFF signifies the feedforward part
of the command signal

The model following variables were calculated from the transformation equations stated in the main body of this report. As mentioned, these equations do not solve for the variables explicitly but use past values on the right hand sides. The error introduced is a time delay of one computer cycle time. For this program, that was 12.5 ms. In other programs that use these transformations the cycle time may be significantly larger and this procedure may not be acceptable. To avoid the additional time delay, the explicit form of the equations is needed. This is given below introducing the three components of V to simplify the expressions.

$$\text{Using } \begin{aligned} u^* &= V^* \cos \alpha^* \cos \beta^* \\ v^* &= V^* \sin \beta^* \\ w^* &= V^* \cos \beta^* \sin \alpha^* \end{aligned}$$

$$\text{then } u_{MF} = u^* + \frac{1}{57.3} (Z_{MTCG}^* q^* - Y_{MTCG}^* r^*)$$

$$v_{MF} = v^* + \frac{1}{57.3} (X_{MTCG}^* r^* - Z_{MTCG}^* p^*)$$

$$w_{MF} = w^* + \frac{1}{57.3} (-X_{MTCG}^* q^* + Y_{MTCG}^* p^*)$$

$$\text{and } V_{MF} = (u_{MF}^2 + v_{MF}^2 + w_{MF}^2)^{1/2}$$

$$\sin \beta_{MF} = \frac{v_{MF}}{V_{MF}}$$

$$\sin \alpha_{MF} = \frac{w_{MF}}{(u_{MF}^2 + w_{MF}^2)^{1/2}}$$

Using the differentiation of the equations above and the fact that $\dot{V}^* = \dot{V}$, $\dot{\alpha}^* = \dot{\alpha}$, and $\dot{\beta}^* = \dot{\beta}$,

$$\text{then } \dot{u}_{MF} = \frac{u^*}{V^*} \dot{V} - v^* \cos \alpha^* \dot{\beta} - w^* \dot{\alpha} + \frac{1}{57.3} (Z_{MTCG}^* \dot{q}^* - Y_{MTCG}^* \dot{r}^*)$$

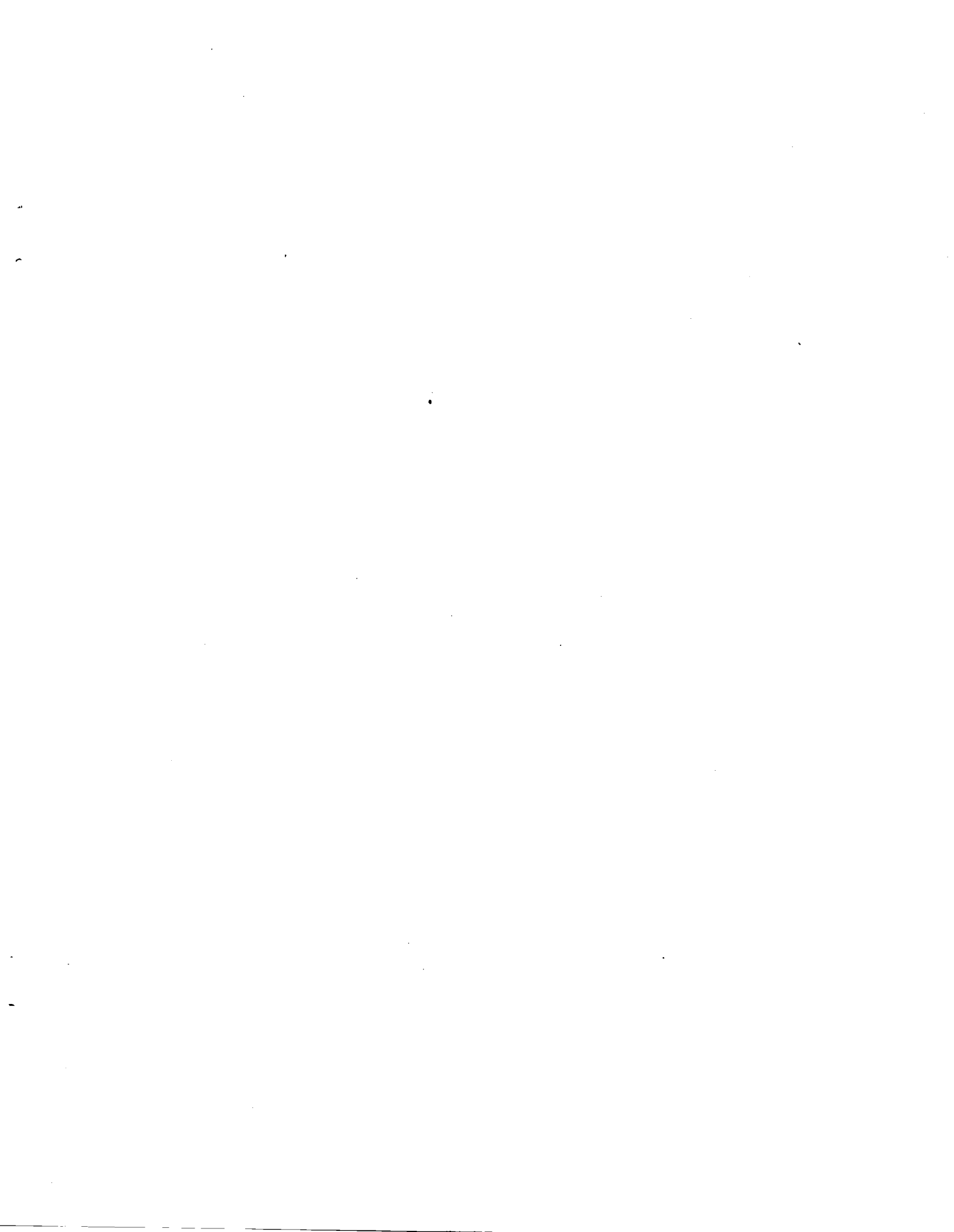
$$\dot{v}_{MF} = \frac{v^*}{V^*} \dot{V} + \frac{u^*}{\cos \alpha^*} \dot{\beta} + \frac{1}{57.3} (X_{MTCG}^* \dot{r}^* - Z_{MTCG}^* \dot{p}^*)$$

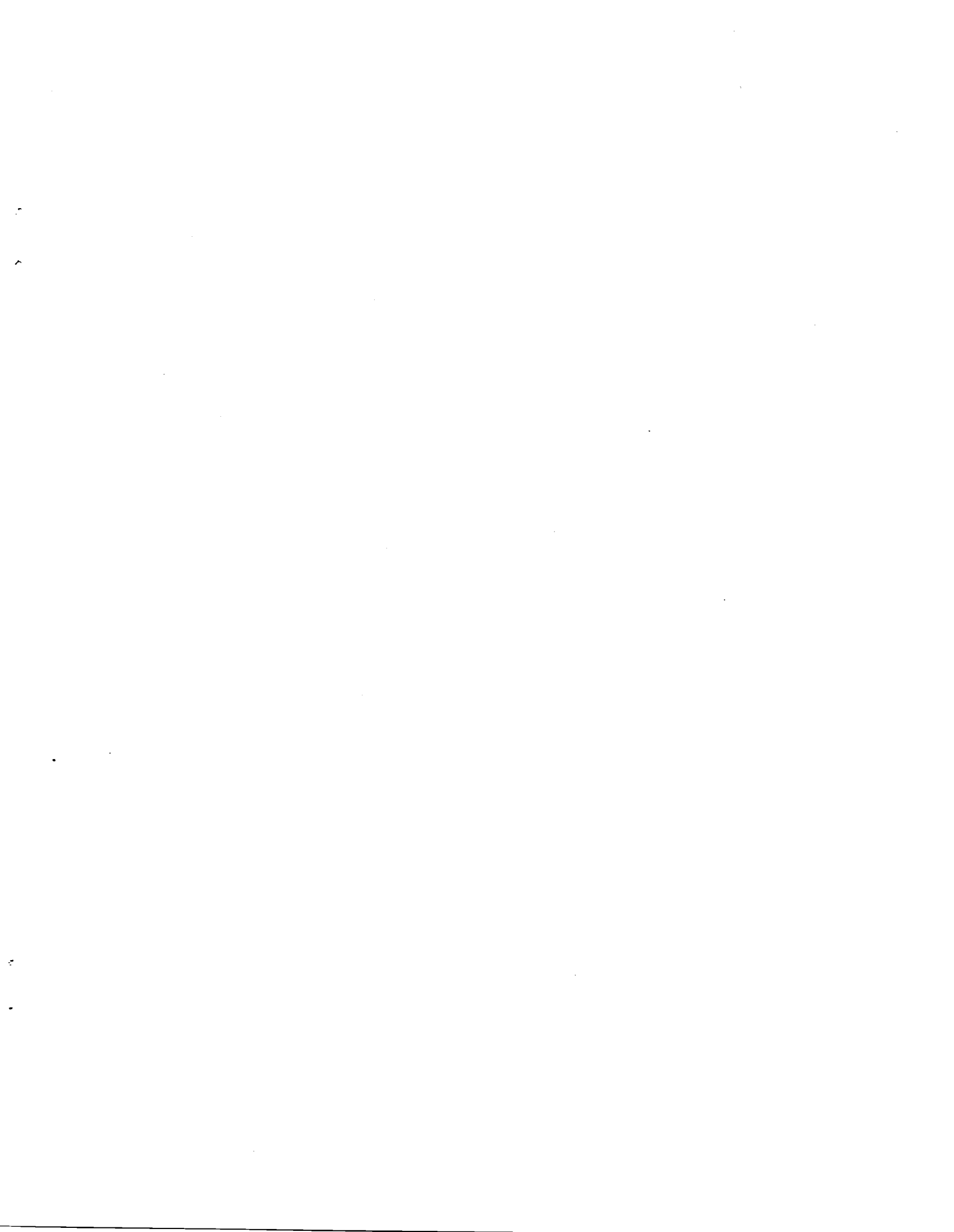
$$\dot{w}_{MF} = \frac{w^*}{V^*} \dot{V} - v^* \sin \alpha^* \dot{\beta} + u^* \dot{\alpha} + \frac{1}{57.3} (-X_{MTCG}^* \dot{q}^* + Y_{MTCG}^* \dot{p}^*)$$

$$\text{Finally, } \dot{V}_{MF} = \frac{u_{MF}}{V_{MF}} \dot{u}_{MF} + \frac{v_{MF}}{V_{MF}} \dot{v}_{MF} + \frac{w_{MF}}{V_{MF}} \dot{w}_{MF}$$

$$\dot{\beta}_{MF} = \frac{57.3}{(u_{MF}^2 + w_{MF}^2)^{1/2}} \dot{v}_{MF} - \frac{57.3 v_{MF}}{V_{MF} (u_{MF}^2 + w_{MF}^2)^{1/2}} \dot{V}_{MF}$$

$$\dot{\alpha}_{MF} = \frac{57.3 w_{MF}}{u_{MF}^2 + w_{MF}^2} \dot{u}_{MF} - \frac{57.3 u_{MF}}{u_{MF}^2 + w_{MF}^2} \dot{w}_{MF}$$







LANGLEY RESEARCH CENTER

3 1176 00518 4727